NASA CR-135156

ANALYSIS AND TESTS OF NASA COVERT GROOVE HEAT PIPE

Grumman Aerospace Corporation
Bethpage, New York

prepared for

NATIONAL AERONAUTICS AND SPACE ADMINISTRATION

Lewis Research Center
Cleveland, Ohio

December 1976

Contract C-65532

1 Report No	2 Government Accession No	3 Recipient's Catalog No
NASA CR-135156		

4 Title and Subtitle	5 Report Date
ANALYSIS AND TESTS OF NASA COVERT GROOVE HEAT PIPE	December 1976
	6 Performing Organization Code
7 Author(s)	8 Performing Organization Report No: None
	10 Work Unit No
9 Performing Organization Name and Address: Grumman Aerospace Corporation, Bethpage, New York 11714	11 Contract or Grant No: C-65532
12 Sponsoring Agency Name and Address: National Aeronautics and Space Administration, Washington, D. C. 20546	13 Type of Report and Period Covered: Contractor Report
	14 Sponsoring Agency Code

15 Supplementary Notes

Final Report. Project Managers, Warner B. Kaufman and Leonard K Tower, Physical Science Division, NASA Lewis Research Center, Cleveland, Ohio

16 Abstract

A low-cost thermal control heat pipe having nearly covered grooves extruded in aluminum has been developed at NASA Analytical predictions of transport capability are in excellent agreement with experimental results using ammonia. Axial heat transport predictions as a function of fluid charge are presented also for methane, ethane, propane, and butane Experimental tests show performance considerably better than that of open groove extruded pipes and comparing favorably with that of more complicated arterial/wick configurations. For ammonia at 20^{o} C, the covert groove pipe obtained a static wicking height of 2.5 cm and an axial heat transport capability of 143 W-m

17 Key Words (Suggested by Author(s))	18 Distribution Statement
Heat pipes; Thermal control; Heat transfer; Heat recovery; Spacecraft thermal control; Extruded tubing	Unclassified - unlimited

19 Security Classif (of this report)	20 Security Classif (of this page)	21 No of Pages	22 Price*
Unclassified	Unclassified	55	A04

* For sale by the National Technical Information Service, Springfield, Virginia 22161

PREFACE

The Lewis Research Center has for some time been interested in heat pipes as an adjunct to thermionic converters for space power production Increasing interest in heat pipes for spacecraft thermal control caused members of the Thermionic and Heat Pipe Section to undertake a familiarization survey and study of such pipes It became evident that existing designs having the simplicity of the grooved pipe had excessive sensitivity to tilt in a 1-g environment and their performance was rather low Pipes with internal configurations designed to overcome these defects were very costly to build. They also suffered from depriming problems in the presence of a noncondensable gas, which might be formed as a consequence of corrosion or might be used as a control gas in a variable conductance heat pipe.

At this point Mr Roland Breitwieser conceived the convert groove heat pipe. Preliminary studies were made of the effects of groove diameter and number and of slot width on pipe performance. For instance, relaxation studies were made to determine roughly the temperature gradient from the groove root to the groove land when these parameters were varied at different heat inputs. This gradient in part is a factor in nucleate boiling in the grooves. Also considered was the effect of groove diameter on the permissible pipe tilt before self-priming became impossible and on the axial heat transport performance limit.

With these very rough studies as a basis, procurement of the most promising configuration within the limits of the extruder's art was negotiated with Micro Extrusions, a division of Universal Alloys Corporation, now in Anaheim, California. The late Mr. Earl Bell of that company lent his enthusiastic support.

After a few tries, Micro Extrusions succeeded in producing a sufficient amount of tubing close to the desired specifications to make the construction and testing of a heat pipe feasible Facilities for manufacture and filling of the pipes did not exist at the Lewis Research Center. A procurement involving these steps together with a detailed analysis of the prospective performance of the configuration was therefore initiated. The work described in this report is the consequence of that procurement.

Warner B. Kaufman
Leonard K Tower

CONTENTS

ILLUSTRATIONS

TABLES

NOMENCLATURE

Symbols

A	area
d	diameter
Delta	parameter used to update axial heat transfer
f	friction factor
F	parameter used to update meniscus radius
g	gravitational constant
N_G	Number of grooves
P	pressure
Q	axial heat transfer
R	meniscus radius
T	temperature
V	velocity
W	groove width
WP	wetted perimeter
X_M	meniscus arc length
x	axial distance
σ	surface tension
θ	groove convergent taper angle
μ	viscosity
λ	latent heat
ρ	density
τ	shear

Suffix

EVAP	evaporator section
ADIA	adiabatic section
COND	condenser section
ℓ	liquid
v	vapor
v/ℓ shear	vapor/liquid shear term
cap	capillary
1, 2	location

SUMMARY

Trade-off studies were performed at NASA Lewis to establish groove profile and dimensions for an axial grooved heat pipe extrusion. The aim of the study was to develop a low-cost, high-performance heat pipe with good ground test characteristics. The study resulted in the selection of a re-entrant groove profile and an extrusion in 6063 aluminum alloy was produced by Micro Extrusions Division, Universal Alloy Corp. of Anaheim, California.

Grumman Aerospace was subsequently awarded a small contract to write a computer code that would predict the performance of the extrusion, then fabricate and test two heat pipes for a comparison of measured performance characteristics and analytical predictions. This report covers the work performed by Grumman Aerospace under this contract.

The main conclusions are:

- The groove profile is very regular with little groove to groove variation and no rifling of the grooves.
- The extrusion exhibits good ground testability features with high static wicking height and good axial pumping capability. For ammonia at 20°C the test data are in good agreement with analytical predictions showing a static wicking height of 25 mm. and an axial heat transport capability of 143 watt meters.
- The measured evaporator and condenser film coefficients are also in good qualitative agreement with what one would predict from previously published data on axially grooved heat pipes. The evaporator and condenser coefficients were 7300 and 20,500 watts per square meter °C respectively, referenced to internal area at core diameter.

1. INTRODUCTION

The first published accounts of the heat pipe principle were by Gaugler (Ref. 1) in 1945 and Thompson (Ref. 2) in 1960. It was not until 1964, however, that Grover et al (Ref. 3) independently realized the potential of the heat pipe principle. Grover's paper was quickly followed by a number of papers deriving the theory of heat pipes (Ref. 4, 5, 6). The initial theoretical approach was an attempt to equate the capillary pumping to the system viscous losses with simplified gravitational effects. For grooved pipes, Frank (Ref. 6) developed an optimization procedure for maximum transport capacity in zero-g based on grooves of specified non-dimensional shape. Recent advances to groove theory include, consideration of real groove geometry (fillets, etc.) with numerical integration along the groove to determine fill requirements for zero-g applications (Ref. 7), visualization of liquid distribution in grooves (Ref. 8), groove-by-groove analysis backed-up by neutron photography to determine puddle characteristics (Ref. 9), inclusion of shear at the liquid/vapor interface (Ref. 10), and zero-g flight data (Ref. 11).

In the early days of the heat pipe the axial grooves were produced by machining or broaching the groove into the inside surface of thick wall tube. It was not until 1967 that Grumman Aerospace working with the French Tube Corp. produced the first practical, low cost grooved heat pipe tubing (Ref. 8). This tubing was produced by a swaging process. Under contract to NASA GSFC Grumman built three isothermalizers from this grooved tubing for the OAO-B spacecraft. (Ref. 9) The working fluid was Freon-21. In a continuous upgrading of the heat pipe performance an additional pipe was built for the OAO-C spacecraft. This pipe had ammonia as working fluid. This pipe is still functioning on the spacecraft after four years in orbit (Ref. 12).

The successful performance of this pipe led NASA GSFC to baseline similar pipes as the prime thermal control system for the ATS-F spacecraft and 55 swaged axial groove ammonia heat pipes were built into the North, South and Transverse panels of the spacecraft (Ref. 13).

Swaged tubing had a number of disadvantages including;

- poor ground testability - the swaging process is a very severe operation and results in poor uniformity (axial and circumferential) in groove dimensions as well as relatively wide grooves.
- poor surface condition. The swaging process invariably results in crevices and can result in inclusions which may not be removed in the cleaning process.

These disadvantages were recognized early by NASA GSFC and as part of the ATS-F program a survey of extrusion houses was made and as a result Micro Extrusions Division of Universal Alloy Corp. of Anaheim, CA, produced an extruded axially grooved tube (Ref. 10). At approximately the same time Battelle Inst. also produced an axially grooved extrusion (Ref. 14), though with somewhat lower transport capacity than the NASA GSFC extrusion.

The NASA GSFC extrusion (referred to elsewhere in the open literature as the Micro Extrusion or as the ATS extrusion) was a considerable improvement over the original swaged tube being cleaner and considerably more uniform. However it still had poor ground testability, that is, it was very tilt sensitive. At this point NASA Lewis performed some trade-off studies on improving the performance of axially grooved heat pipes, particularly to improve static wicking height without significantly reducing transport capability. The result of these trade-off studies was the NASA Lewis Covert Groove extrusion.

Only a few lengths of this extrusion were produced for test purposes. This report details the analysis and testing of this extrusion.

2. ANALYTICAL MODEL

The effort included in this phase of the program consisted of determining the characteristic shape of the axial grooves, writing a computer code to estimate the transport capability of the extrusion and finally exercising the computer code parametrically to predict the transport capability of the extrusion with various fluids, ranging from ammonia at room temperature to methane at 100K.

2.1 Characteristic Dimensions

Three lengths of extrusion were examined in this investigation, each length being approximately 0.9M (3 ft) long. The initial examination consisted of measuring the pipe outside diameter at ten randomly selected locations along and around each pipe length. The raw data are presented in Table I. The data show that pipe length #1 is non-circular and has a smaller diameter than either length #2 or #3. At first it was thought that length #1 had been flattened or squashed. The dry, clean weight per unit length of each pipe length was then determined (Table I). The unit weight of pipe length #1 was 3% less than the corresponding data for lengths #2 or #3. This 3% difference in weight is statistically significant and eliminated the possibility of length #1 being simply flattened.

Next, the pipe internal volume was determined by carefully filling each length of extrusion with water. The internal volume for all three pipe lengths were within 0.4% of each other. This eliminated the possibility of length #1 being squashed but suggested that length #1 had a thinner wall than the other two pipe lengths. It was decided therefore to use length #1 for burst tests and build heat pipes from lengths #2 and 3.

Two cm. (3/4 inch) long samples were cut from each end of lengths #2 and #3. These samples were tagged for traceability and the outside diameter of each sample measured across four different diameters. These small samples were then mounted in an epoxy and polished to expose the sharp groove profile. Photographic enlargements of two of the samples are shown in Figure 1, the full tube shot is

shown at approximately 6 times magnification, the single grooves at approximately 70 times magnification. The tubes have twenty internal, longitudinal grooves, each groove consisting of an entrance passage plus a circular trough. Visual examination of the pipe lengths did not show any rifling or axial twisting of the grooves.

Table I Pipe Parameters

PARAMETER		PIPE #1	PIPE #2	PIPE #3
PIPE OUTSIDE DIAMETER, INCHES	LOCATION # 1	4951	4992	4994
	2	4978	4995	4991
	3	4983	4991	4988
	4	4956	4984	4989
	5	4987	4986	4998
	6	4954	4985	4989
	7	4985	4984	4992
	8	4986	4991	4987
	9	4958	4985	4996
	10	4955	4987	4988
	AVERAGE	4969	4988	4991
	MAXIMUM	4987	4995	4998
	MINIMUM	4951	4984	4987
PIPE LENGTH, INCHES		34 437	33.937	34 563
DRY WEIGHT, GRAMS		103 7	105 2	107 3
DRY WEIGHT/FOOT GM/FT		36 14	37 20	37 25
WEIGHT OF WATER TO FILL PIPE, GRAMS		71 25	69 9	71 5
*INTERNAL VOLUME/FT, CUBIC CM/FT		24 83	24 72	24 82

*BASED UPON DENSITY OF WATER OF 1 GM/CUBIC CM

NOTE ALL LINEAR DIMENSIONS WERE ORIGINALLY RECORDED IN INCHES, HENCE ALL DIMENSIONS TABULATED ABOVE ARE IN INCHES OR FEET THE AVERAGE VALUES OF THE CHARACTERISTIC DIMENSIONS WERE COMPUTED AND ARE GIVEN IN TABLE IV IN INCHES WITH THE CORRESPONDING METRIC VALUES

Photo enlargements showing the pipe cross-section were produced from the mounted samples in two stages, six times magnification negatives, which were subsequently blown-up to give a twenty times magnification print on Mylar. The characteristic dimensions of the pipes and grooves were then measured under an

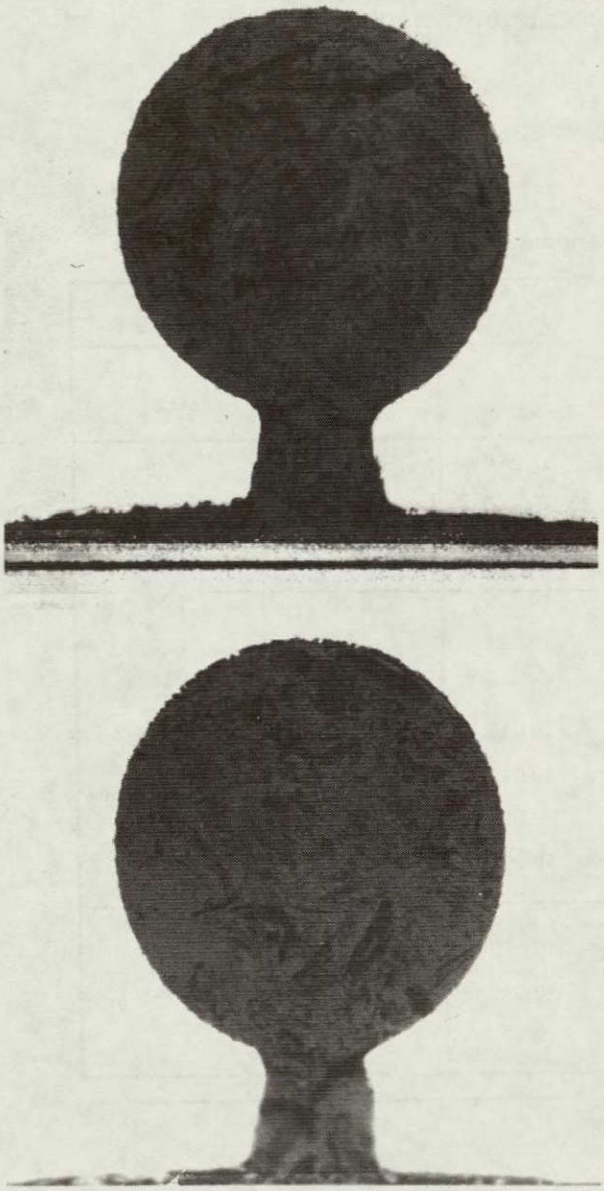

SINGLE GROOVE

MAG ~ 70X

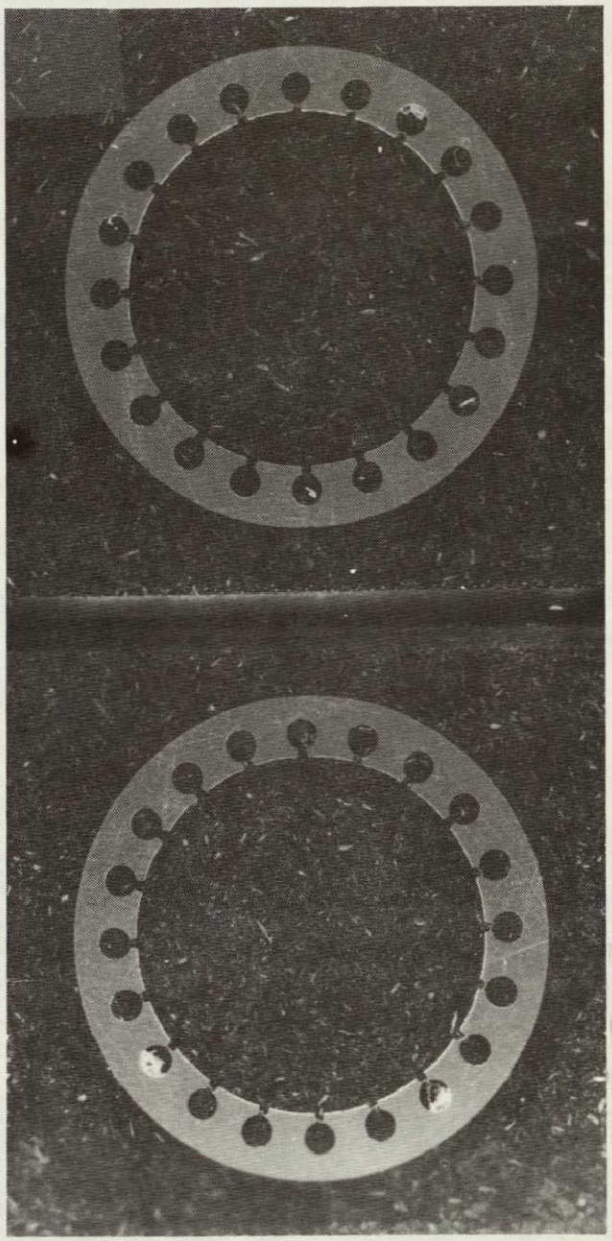

PIPE X-SECTION

MAG~6X

Fig. 1 Photographic Enlargements of Covert, Axially Grooved Extrusion

additional ten power microscope. The raw data are reported in Tables II and III and the reduced data in Table IV. It should be noted that the average values reported are the simple arithmetic average while the "min" and "max" are the minimum and maximum values measured. The characteristic dimensions are explained in Figure 2.

The significant points to be noted from the data are the following.

1. The pipe wall indicates that the core is eccentric by approximately 0.05 mm. This appears to be a true eccentricity. This in itself is not important other than that it increases the local hoop stress.

Table II Covert Groove Dimensions

GROOVE PAIR	PIPE NO. 2*			PIPE NO. 3*		
	D_O	D_R	D_C	D_O	D_R	D_C
1/11	9.95	8.90	7.275	10.01	8.94	7.33
2/12	9.935	8.88	7.250	10.00	8.97	7.33
3/13	9.93	8.90	7.265	10.02	8.99	7.34
4/14	9.945	8.92	7.275	10.035	9.06	7.34
5/15	9.97	8.97	7.320	10.035	9.02	7.33
6/16	9.985	8.97	7.320	10.035	9.00	7.33
7/17	10.000	8.995	7.330	10.015	9.03	7.345
8/18	10.000	9.01	7.350	10.015	8.96	7.32
9/19	10.005	8.975	7.335	9.99	8.97	7.33
10/20	10.97	8.96	7.300	10.00	8.935	7.31
AVG	9.969	8.948	7.302	10.015	8.988	7.331
MAX	10.005	9.01	7.350	10.035	9.06	7.345
MIN	9.93	8.88	7.25	9.99	8.935	7.31
MAGNIFICATION FACTOR		19.986			20.066	

* ALL DIMENSIONS IN INCHES.

NOTE: ALL LINEAR DIMENSIONS WERE ORIGINALLY RECORDED IN INCHES, HENCE ALL DIMENSIONS TABULATED ABOVE ARE IN INCHES OR FEET. THE AVERAGE VALUES OF THE CHARACTERISTIC DIMENSIONS WERE COMPUTED AND ARE GIVEN IN TABLE IV IN INCHES WITH THE CORRESPONDING METRIC VALUES.

2. The individual grooves are not circular and some are off-set (skewed) about their respective entrance passageway. This off-set will have no effect on the groove pumping capability.

3. Most significantly, the groove entrance passageway is convergent.

The internal free cross-sectional area of each of the 2 pipes was computed in

Table IV Summary

BRITISH UNITS (INCHES)							
PARAMETER		PIPE #2			PIPE #3		
		MIN	AVG	MAX	MIN	AVG	MAX
OUTSIDE DIAMETER	D_O	4969	4988	5006	4979	4991	5001
ROOT DIAMETER	D_R	4443	4477	4508	4453	4479	4515
CORE DIAMETER	D_C	3628	3654	3678	3643	3653	3650
ENTRANCE WIDTH	W_T	0094	0105	0122	0087	0106	0128
GROOVE OPENING	W_B	0073	0086	0095	0075	0089	0101
GROOVE DIAMETER	D_{G_1}	0312	0318	0325	0318	0325	0333
	D_{G_2}	0308	0314	0319	0310	0316	0321
	D_{G_3}	0311	0319	0324	0315	0320	0331
WALL THICKNESS	W_{ALL}	0245	0252	0273	0232	0253	0277
METRIC UNITS (MM)							
PARAMETER		PIPE #2			PIPE #3		
		MIN	AVG	MAX	MIN	AVG	MAX
OUTSIDE DIAMETER	D_O	12 62	12 67	12 72	12 65	12 68	12 70
ROOT DIAMETER	D_R	11 29	11 37	11 45	11 31	11 38	11 47
CORE DIAMETER	D_C	9 22	9 28	9 34	9 25	9 28	9 27
ENTRANCE WIDTH	W_T	239	267	309	221	269	325
GROOVE OPENING	W_B	185	218	241	191	226	256
GROOVE DIAMETER	D_{G_1}	792	808	826	808	826	846
	D_{G_2}	782	798	810	787	803	815
	D_{G_3}	790	810	823	800	813	841
WALL THICKNESS	W_{ALL}	622	640	693	589	643	704

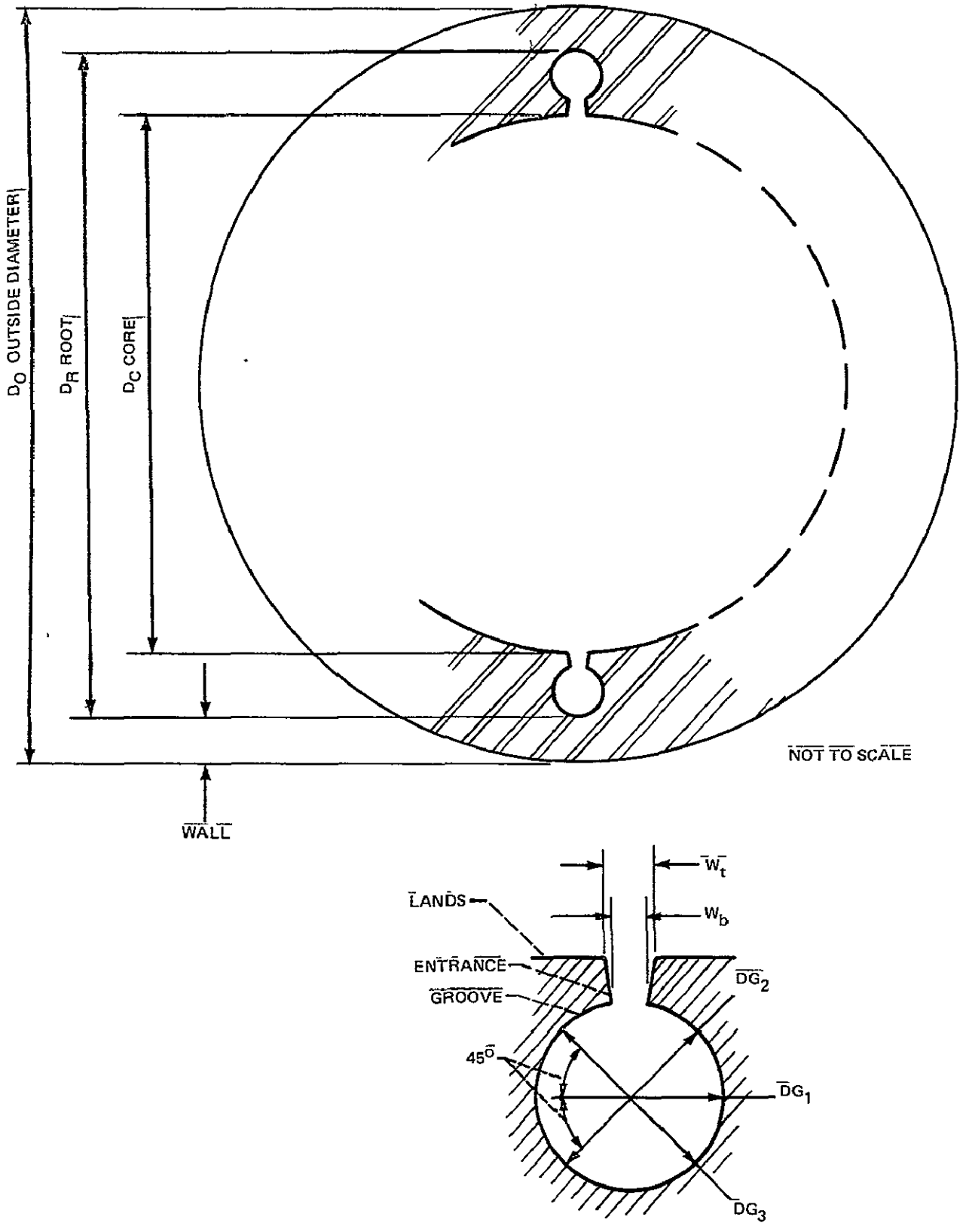

Fig 2 Covert Groove Characteristic Dimensions

3 ways:

- from the accurately known pipe outside diameter, length and weight;
- from the volume of water required to fill each pipe;
- from the measured (average) dimensions;

the computed internal cross section areas being 0.8110, 0.8129 and 0.7910 cm^2 respectively (0.1257, 0.1260 and 0.1226 in^2). In addition the average taper of the entrance passageway was calculated as 5 degrees 46 minutes.

2.2 Computer Program

A simple computer program was written to evaluate the zero gravity heat transport capability of the Lewis covert, axially grooved heat pipe extrusion. This computer program was based upon hydrodynamic phenonoma, all thermodynamic processes being ignored. As is usual with heat pipe analysis, the starting point was to assume a pressure balance;

$$\Delta P_{cap} = \Delta P_{\ell} + \Delta P_{v} + \Delta P_{v/\ell \text{ shear}}$$

where ΔP_{cap} is the capillary pressure difference

ΔP_{ℓ} the liquid phase pressure drop

ΔP_{v} the vapor phase pressure drop

$\Delta P_{v/\ell \text{ shear}}$ is the additional pressure drop in the liquid phase due to the countercurrent vapor flow.

The heat pipe was broken up into a number of axial elements and, starting at the evaporator end, the pressure balance is applied to each element in turn.

The following assumptions were used in deriving the governing equations:

1. All grooves had the average groove geometry with no axial or circumferential variation.

2. Uniform circumferential and axial heat input and rejection.

3. One dimensional laminar flow in the liquid phase (grooves).

4. One dimensional laminar or turbulent flow in the vapor phase (core).

5. Local one dimensional curvature of the meniscus.

The maximum capillary pressure which can be sustained by the groove is given by

$$\Delta P_{cap} = \frac{2.\sigma \cdot \cos \theta}{W}$$

where σ is the surface tension

W the minimum groove opening

θ the combined effect of the groove taper and the fluid, surface wetting angle.

The liquid flow in the grooves, in all cases of interest, is in the laminar regime. Neglecting flow in the radial direction and equating the pressure drop in the circular groove to the pressure drop in the entrance gap then the Fanning Equation gives

$$\Delta P_{\ell} = \frac{2.\mu_{\ell}}{g.\lambda.\rho_{\ell}.N_G} \cdot \left[\frac{1}{\frac{A_1^3}{WP_1^2} + \frac{A_2^3}{WP_2^2}} \right] \cdot Q_{(x)} \cdot dx$$

The vapor flow in the core of the pipe can be in one of three possible regimes,

- laminar (Reynolds Number less than 2300)
- transition (Reynolds Number between 2300 and 3900)
- turbulent (Reynolds Number above 3900)

The variation of friction factor with Reynolds Number can then be idealized as shown on Figure 3. This three regime approach eliminates the abrupt discontinuty in friction factor, Reynolds Number relationship inherent in a two regime approach. Again applying the Fanning friction factor equation

$$\Delta P_v = \frac{4f}{d} \cdot \frac{\rho V^2}{2g} \cdot \Delta x$$

where f is a function of Reynolds number as defined above.

To evaluate the vapor, liquid shear term the basic equations for shear were used;

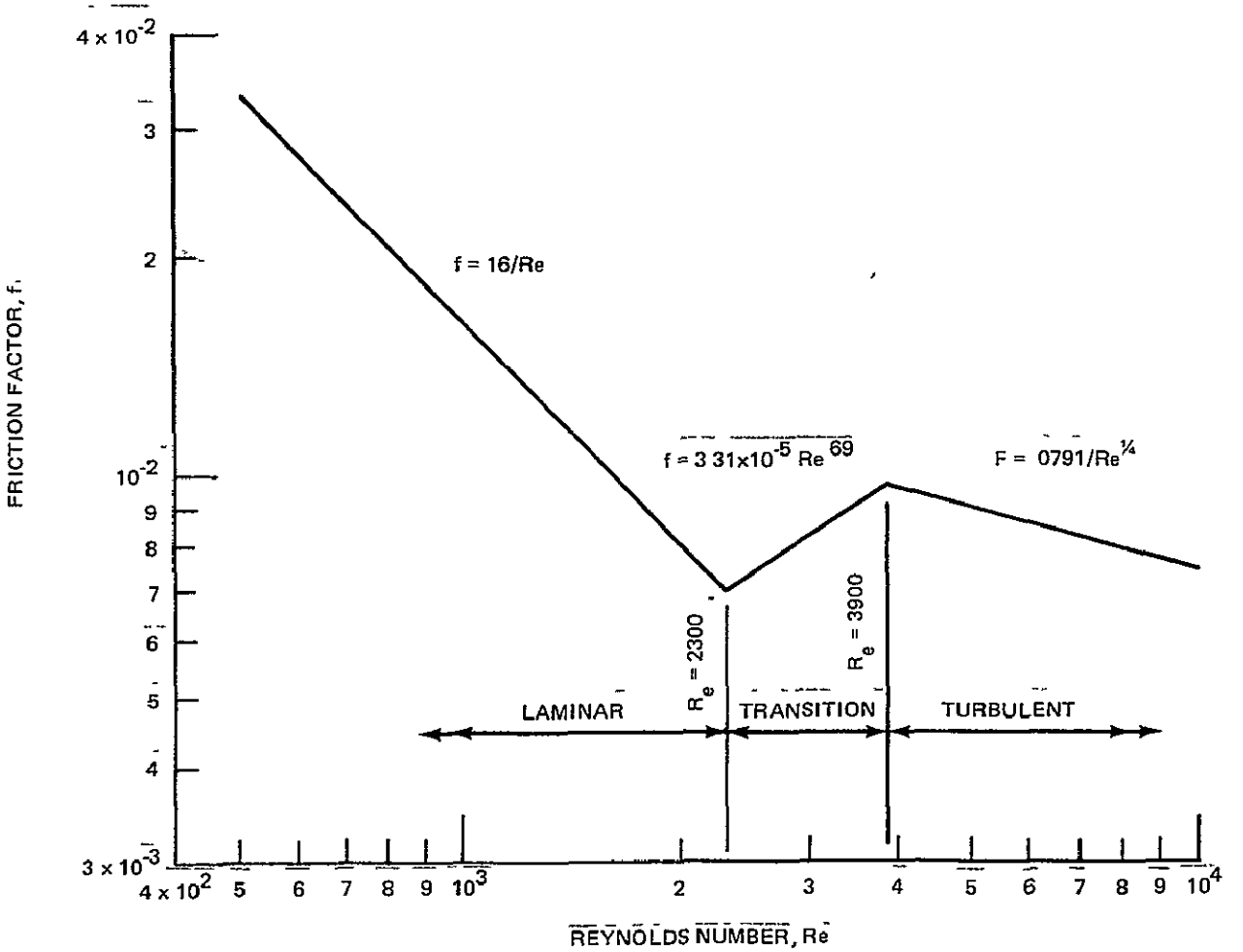

Fig 3 Assumed Variation of Friction Factor With Reynolds Number

$$\bar{A}_{\ell} \cdot \bar{\Delta P}_{v/\ell\,shear} = \tau \cdot X_M \cdot \overline{\Delta x}$$

$$A_v \cdot \Delta P_v = \tau \cdot WP_v \cdot \Delta x$$

hence the shear term can be simply expressed as a function of the vapor pressure drop

$$\Delta P_{v/\ell\,shear} = \Delta P_v \cdot \left(\frac{X_M}{WP_v}\right)\left(\frac{A_v}{A_\ell}\right)$$

where X_M and WP_v are the arc lengths of the meniscus and the wetted perimeter of the vapor space, respectively.

The program was set-up to divide the pipe into a number of axial elements and integrate along the element. The meniscus radius of curvature at the end of the evaporator is set (either at the minimum value or greater) and the variation of the meniscus radius along the pipe calculated. At each step the meniscus radius was examined until the meniscus became flat. If the meniscus at the end of the condenser was depressed then the program increments the axial heat transport and repeats the integration. If the meniscus is flat this corresponds to dry-out for the assumed conditions and a new value of radius of curvature of the meniscus at the end of the evaporator is assumed and the integration process repeated. A typical map generated from the program output data is shown in Figure 4. This figure can be explained:

- Line ABC corresponds to minimum radius of curvature in the evaporator with the meniscus radius at the end of the condenser becoming less depressed as you move along the curve from A to C.
- At point C the meniscus in the condenser is flat and in the evaporator fully depressed.
- The program then returns to point A′ and generates data for curve A′C′ starting with a less depressed meniscus in the evaporator.

- The locus of Point C, C^1, C^2 (i.e., curve CDE) represents a flat meniscus

in the condenser and partially depressed meniscus in the evaporator, the evaporator meniscus becoming flatter as you move along the curve from C to E.

- Point C represents the maximum pumping capability of the pipe with a fully depressed meniscus in the evaporator and a flat meniscus in the condenser.

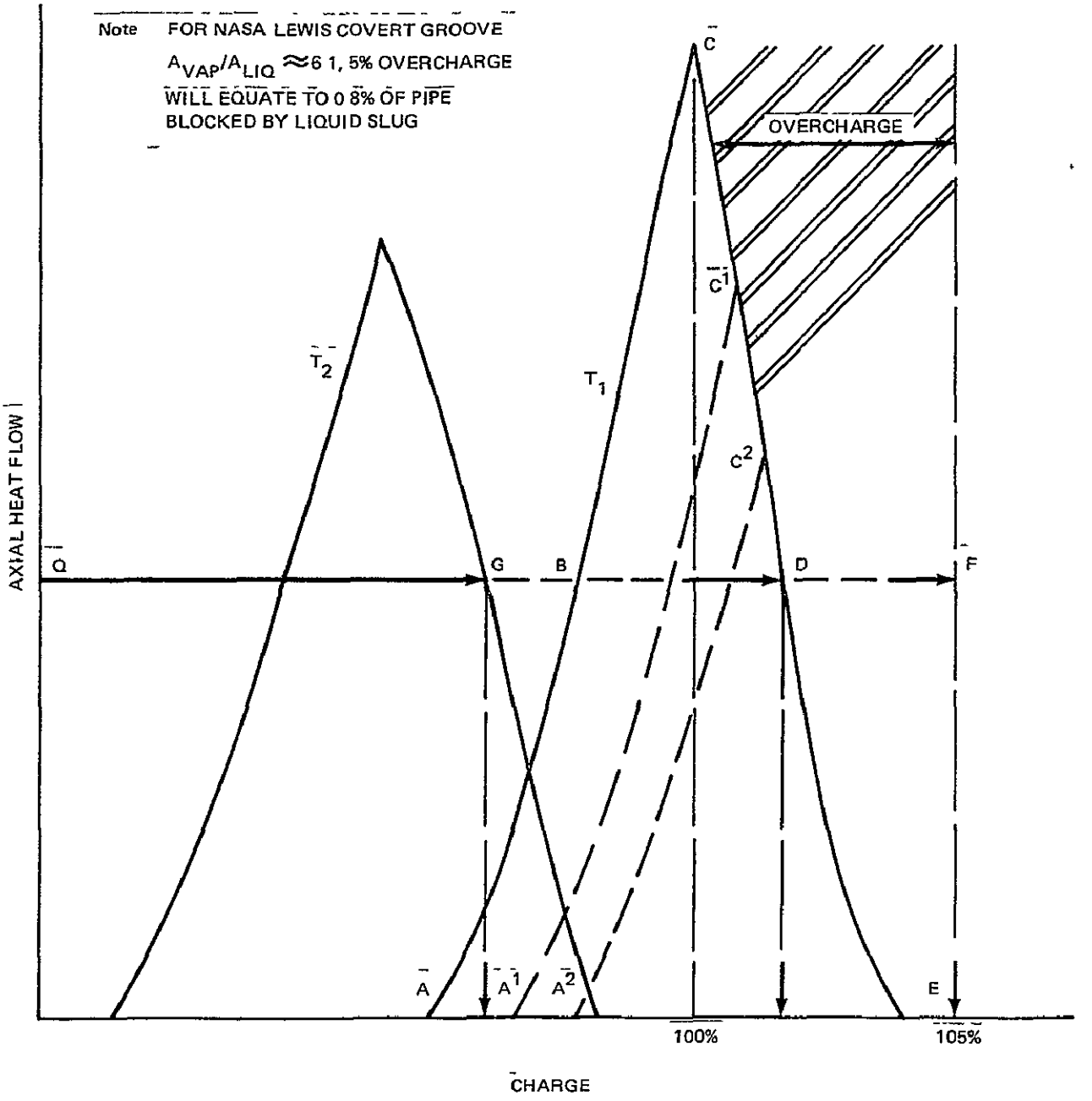

Fig 4 Typical Charge/Performance Map

A pipe can be operated at a low axial heat transport (Q) over a range of charge conditions (BD). With any charge below B the pipe will dry-out at Q watts. With any charge above D the pipe will be overcharged and a liquid slug will form.

Normally one would charge a pipe for maximum pumping capability at a given temperature (Point C temperature T_1). The tolerance on the charge would typically be +5%, -0%. If the pipe is now operated at some lower axial heat transport, at the same temperature, then the overcharge condition will decrease (DF). If the temperature changes to T_2, then the overcharge will also change (GF).

Additional parameters are evaluated in the program including static wicking height, sonic heat flux and entrainment limit.

A listing of the program input data and a sample output are given in the appendix.

2.3 Analytical Results

The computed performance map for the covert groove with ammonia at 20°C is presented in Figure 5. Three conditions have been shown, predictions for nominal groove dimensions and predictions for toleranced dimensions where the dimensions have been stacked to increase or decrease the performance. A point to note from this figure is the sensitivity of performance to undercharge. (Overcharge does not cut performance, but results in some condenser blockage.)

In Figure 6 the performance of the covert groove with nominal dimensions and ammonia had been presented over a range of operating temperatures. The interesting point in this figure is the locus of peak performance points. This shows that as the temperature increases the fluid charge for maximum performance initially decreases then starts to increase again. This is due to the large vapor to liquid volume ratio of the covert groove (approx. 6·1). This variation in required charge is also shown in Figure 7. Taking the required charge at 0°C as 100% then the required charge decreases to a minimum of 98.5% at 30°C then increases again, that is, the overcharge condition would first increase as the temperature increased

from 0^{o}C to 30^{o}C and then decrease past 30^{o}C. It should be noted that with the NASA LEWIS Covert Groove configuration a 6% overcharge is equivalent (in zero g) to a liquid slug filling 1% of pipe length.

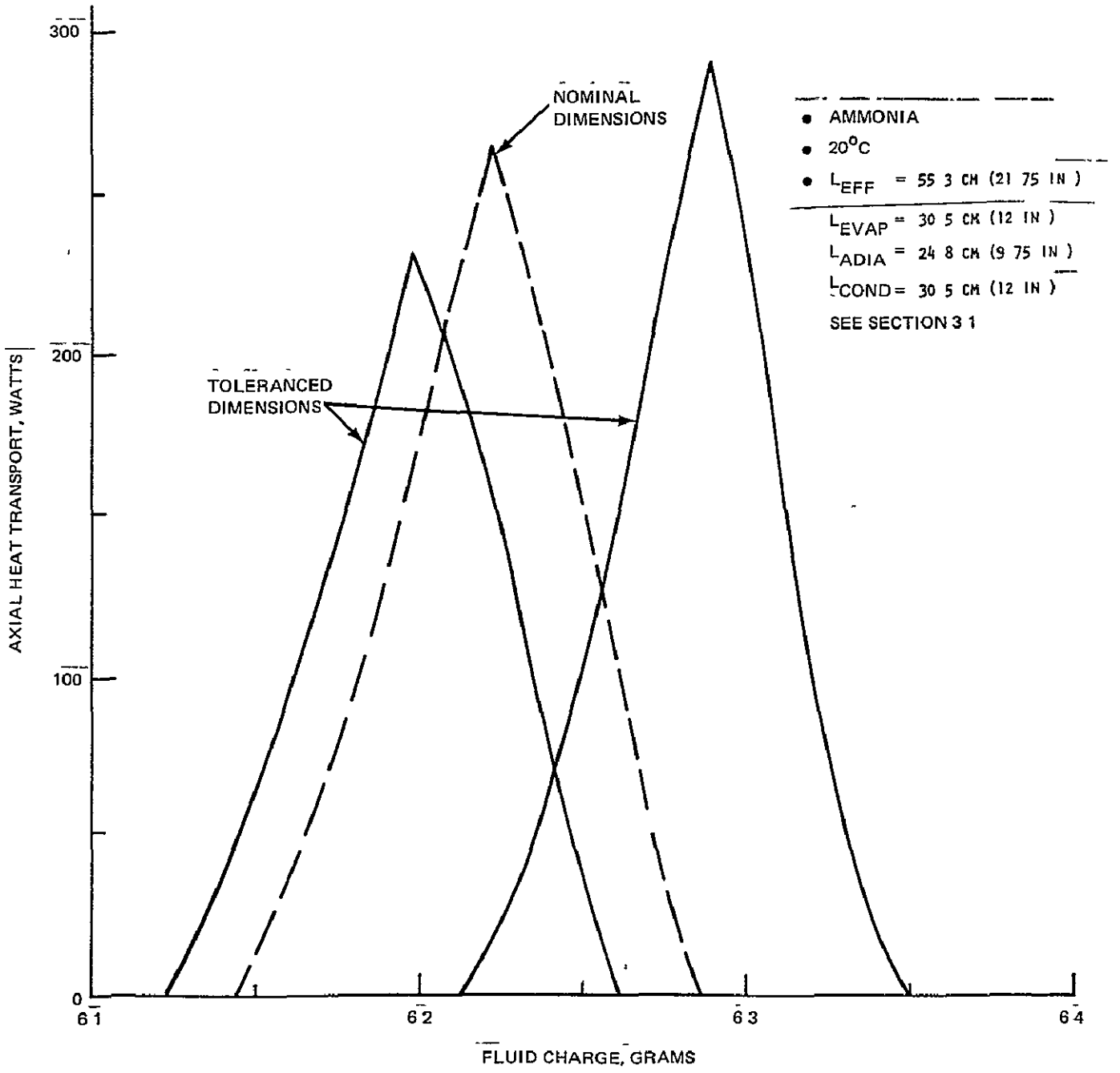

Fig 5 Effect of Measured Groove Dimensional Tolerances

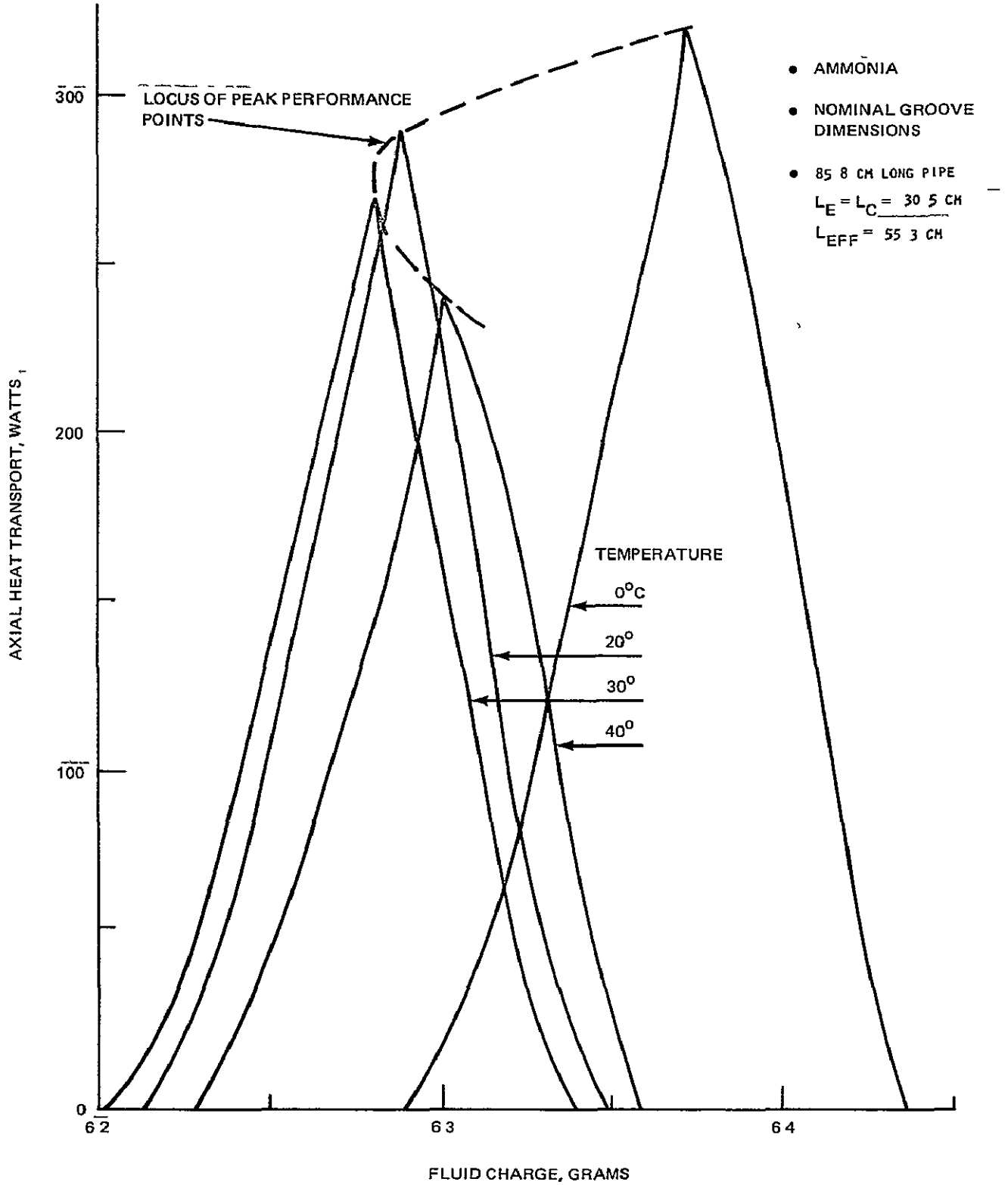

Fig 6 Performance Map for Ammonia Working Fluid

The charge, performance characteristics of the covert groove extrusion with methane, ethane, propane and butane are presented in Figures 8 to 11 and summarized in Table V. In predicting the performance the pipe length was taken as 85.8 cm long, with 30.5 cm evaporator and condenser length and 24.8 cm long adiabatic section.

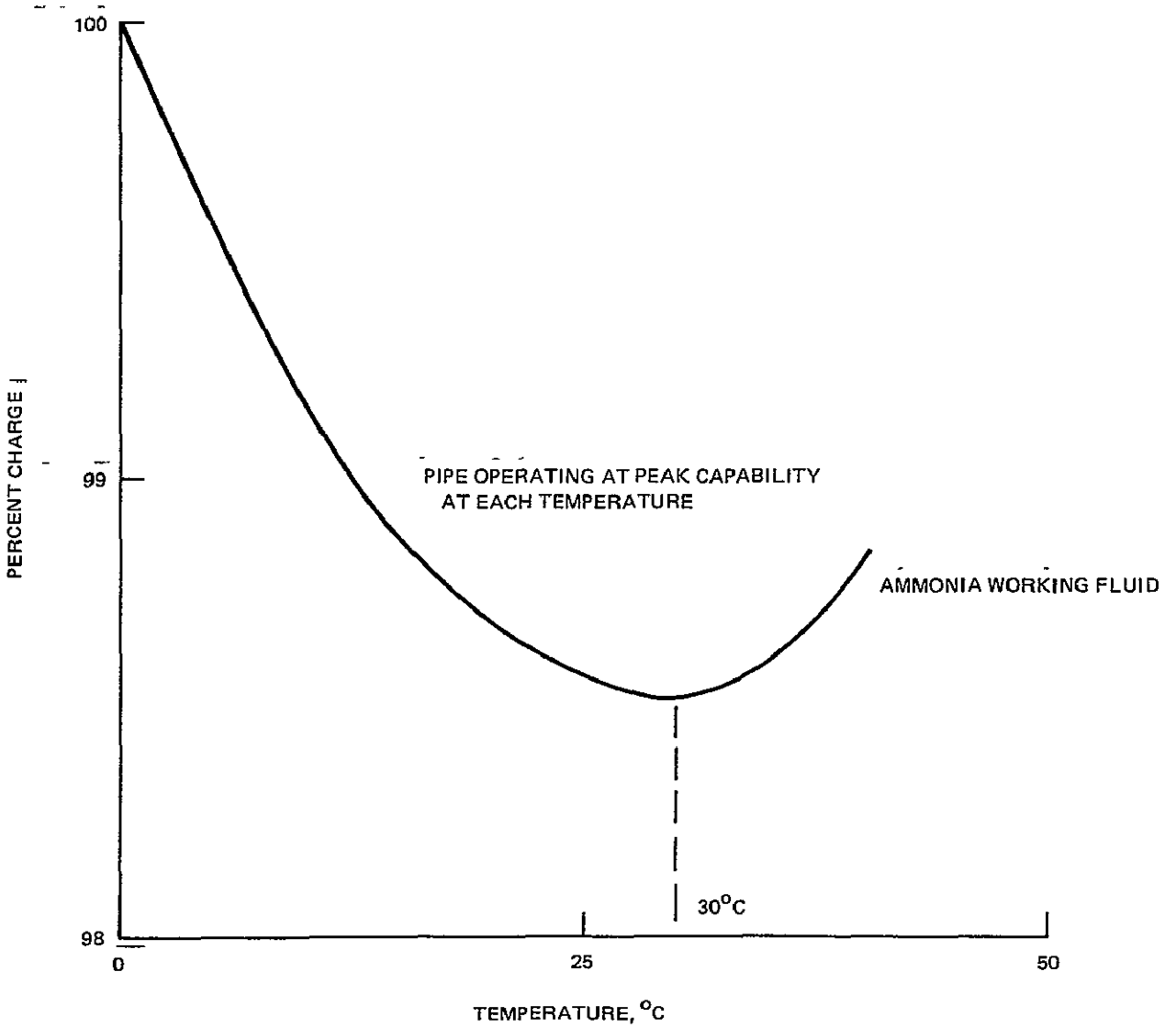

Fig 7 Variation of Fluid Charge With Temperature

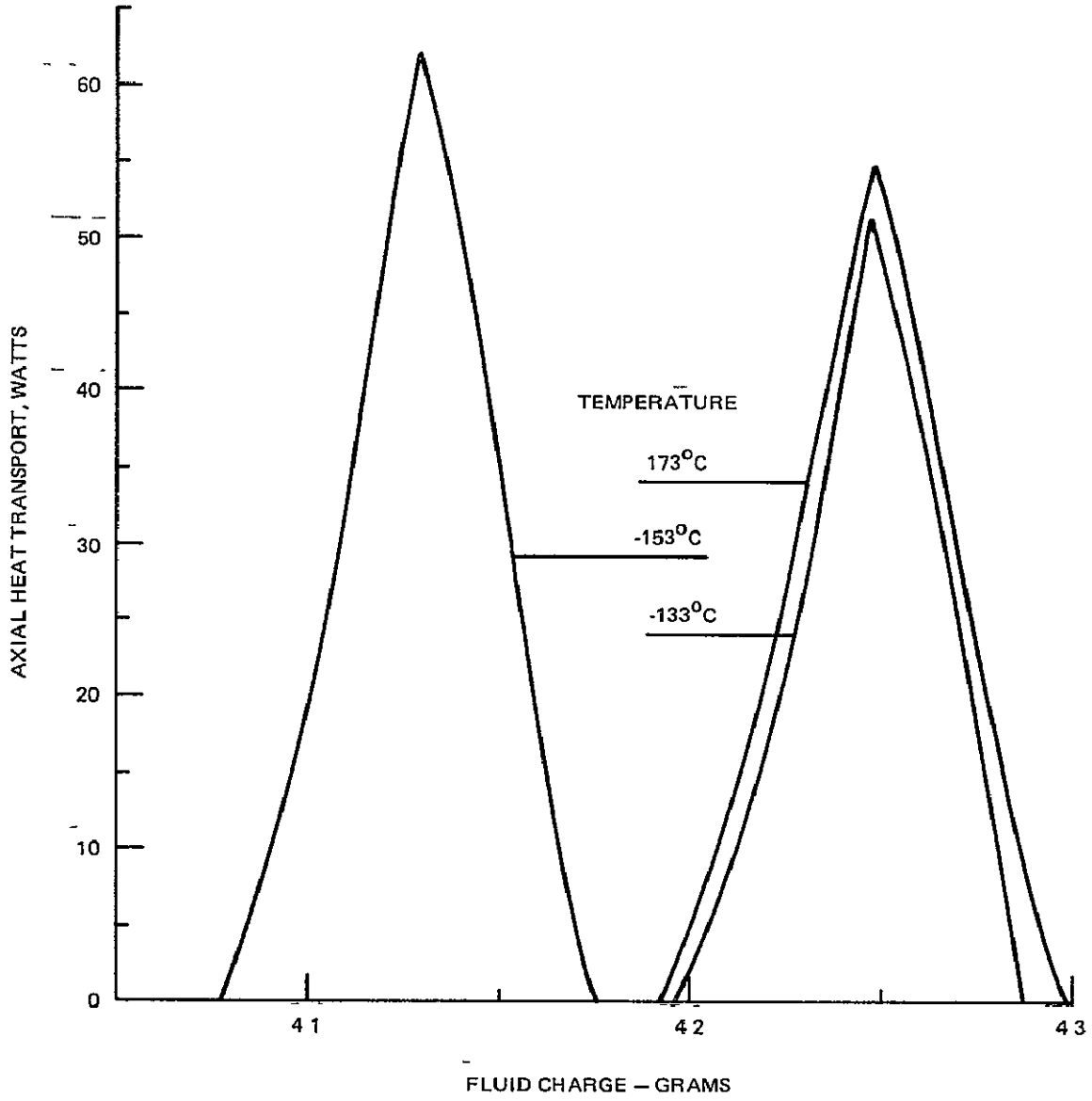

Fig 8 Performance Map for Methane Working Fluid

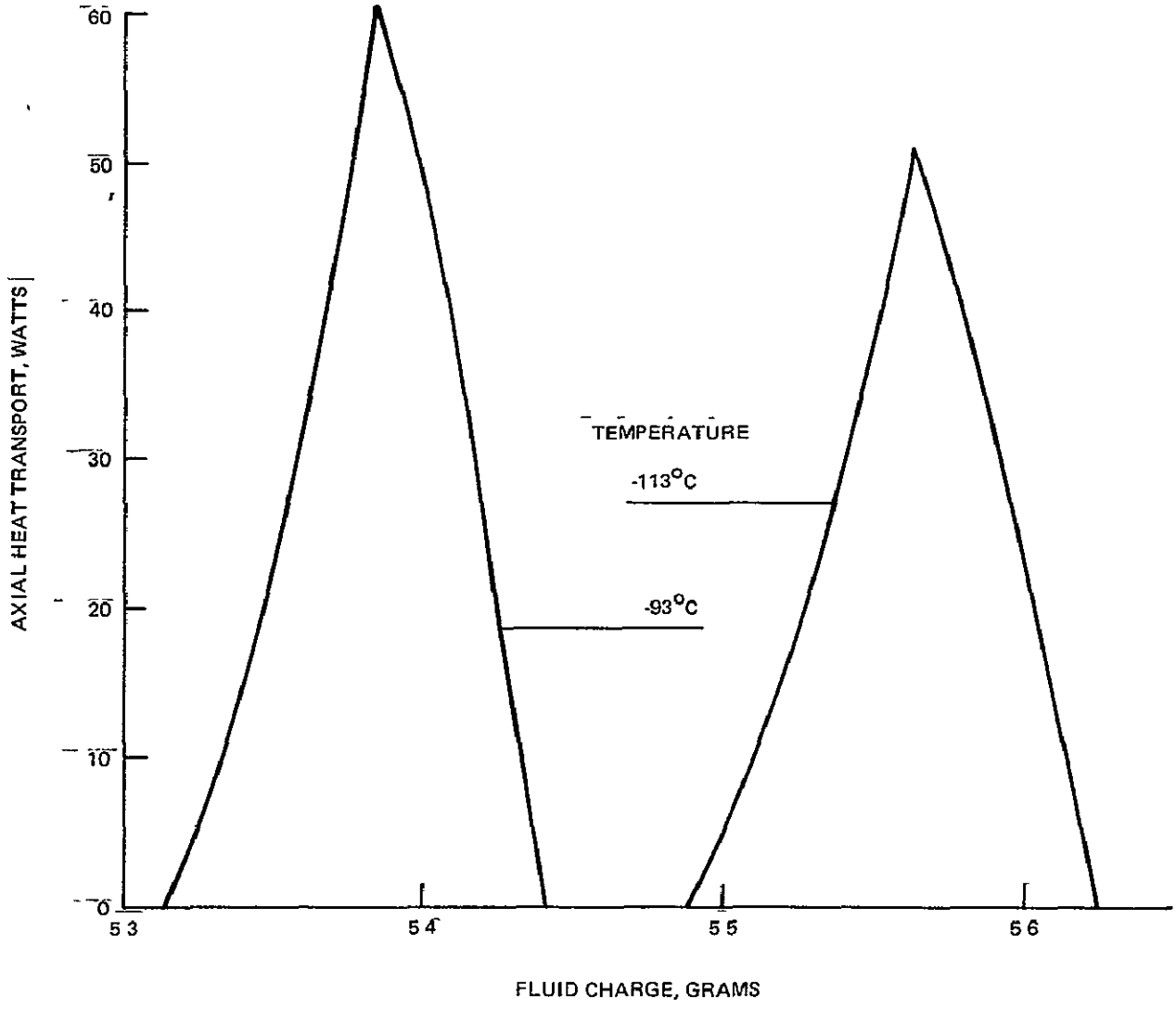

Fig 9 Performance Map for Ethane Working Fluid

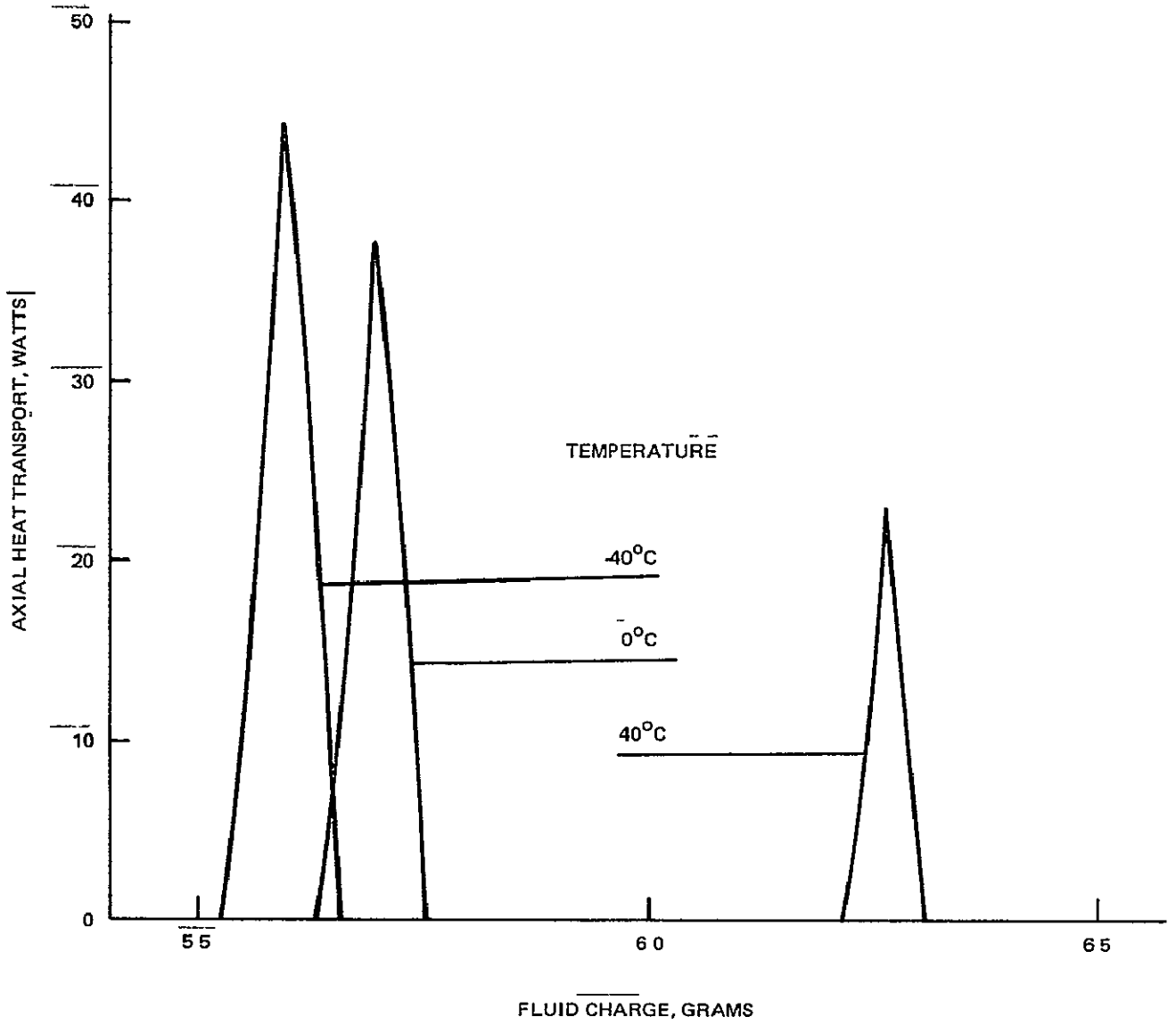

Fig 10 Performance Map for Propane Working Fluid

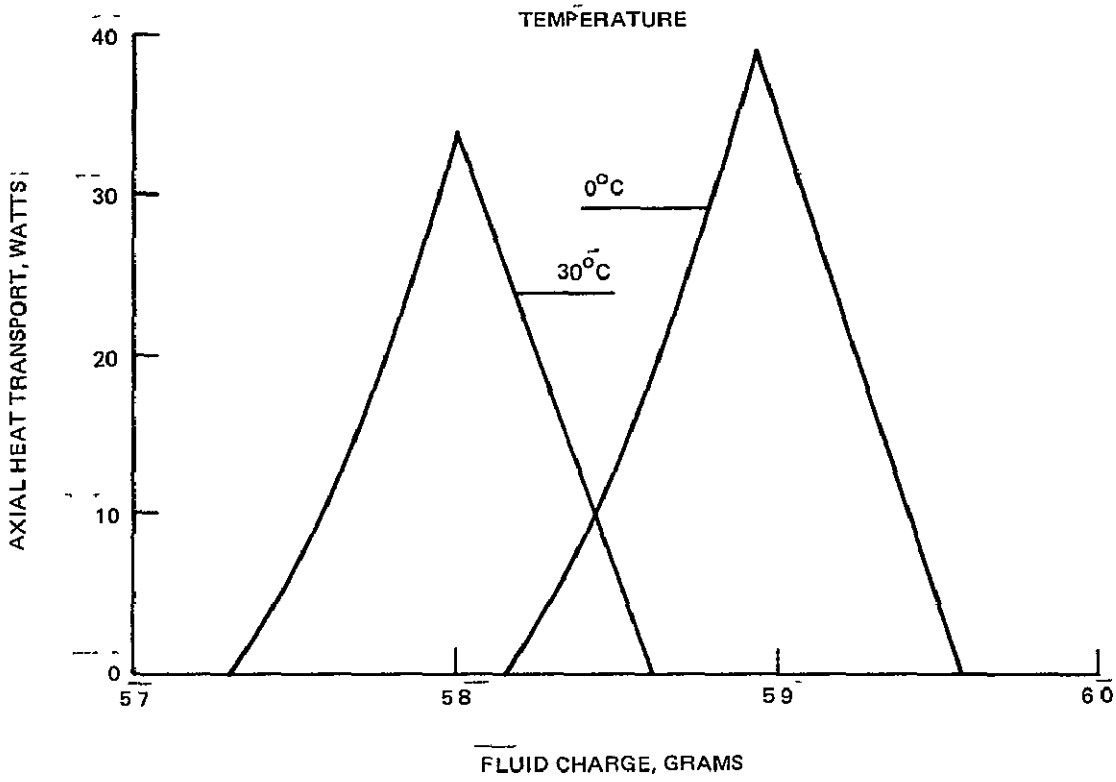

Fig 11 Performance Map for Butane Working Fluid

Table V Summary of Performance Characteristics

FLUID	TEMP, °C	MAX PERFORMANCE POINT			STATIC WICKING HEIGHT, CM
		CHARGE, GMS	TRANSPORT		
			WATTS	WATT M	
AMMONIA	0	6 30	290	160	2 95
	20	6 22	260	143	2 51
	30	6 21	240	132	2 29
	40	6 24	220	121	2 065
METHANE	−173	4 25	55	30	2 71
	−153	4 13	62	34	2 13
	−133	4 25	51	28	1 54
ETHANE	−113	5 56	50	27	2 56
	-- 93	5 38	60	33	2 21
PROPANE	− 40	5 60	45	25	1.95
	0	5 70	38	21	1 36
	40	6 27	23	13	0 81
BUTANE	0	5 88	39	21	1 78
	30	5 80	34	19	1 46

3. EXPERIMENTAL

In this phase of the program two heat pipes were fabricated from the NASA Lewis covert, axially grooved extrusion. Detailed performance characteristics for one of these heat pipes were then experimentally determined with ammonia as the working fluid. These performance characteristics included transport capability as a function of adverse tilt and fluid charge and limited reprimimg tests.

3.1 Heat Pipe Design

The burst pressure of the extrusion was determined using the pipe length designated #1. As previously mentioned, this pipe length was thinner walled than the other two pipe lengths and therefore it was considered that this length of tube would give somewhat pessimistic burst pressure data (approximately 5 to 10% low). Two 230 mm (9 inch) long burst samples were cut from each end of this pipe. One end of each burst sample was capped using flared fittings while the other end was coupled to a hydraulic test facility again using flared fittings. Both samples burst at 190 $\pm$ 6.8 atmospheres, (2800 $\pm$ 100 psig). This is in good agreement with the calculated burst pressure for the extrusion in the T6 temper. Both samples failed by a longitudinal rip along the base of a groove. Coincidentally, both failures initiated approximately two inches from the capped ends. The burst pressure in the TO (as welded) condition was calculated at 54 atmospheres (800 psi). The maximum allowable design pressure would therefore be 47.7 atmospheres (700 psi) in the T6 condition (assuming re-heat treatment after welding on end caps), and 13.6 atmospheres (200 psi) in the TO condition (using the pipe in the as-welded condition).

Assuming the pipe is 5% overcharged with ammonia at 0^{o}C then the maximum operating temperature would be limited to 36^{o}C in the as-welded condition and 85^{o}C in the T6 condition. On increasing temperature the liquid phase would disappear at 124^{o}C and 92 atmospheres and any further increase in temperature would increase the degree of superheat of the vapor with a pressure of 190 atmospheres corresponding to 235^{o}C. To ensure reasonable working margins, it was decided to heat treat the

pipe to the T-6 condition. The details of the end fittings are given in Fig. 12. Seal rings were used to seal the ends of the grooves to prevent end wall drainage.

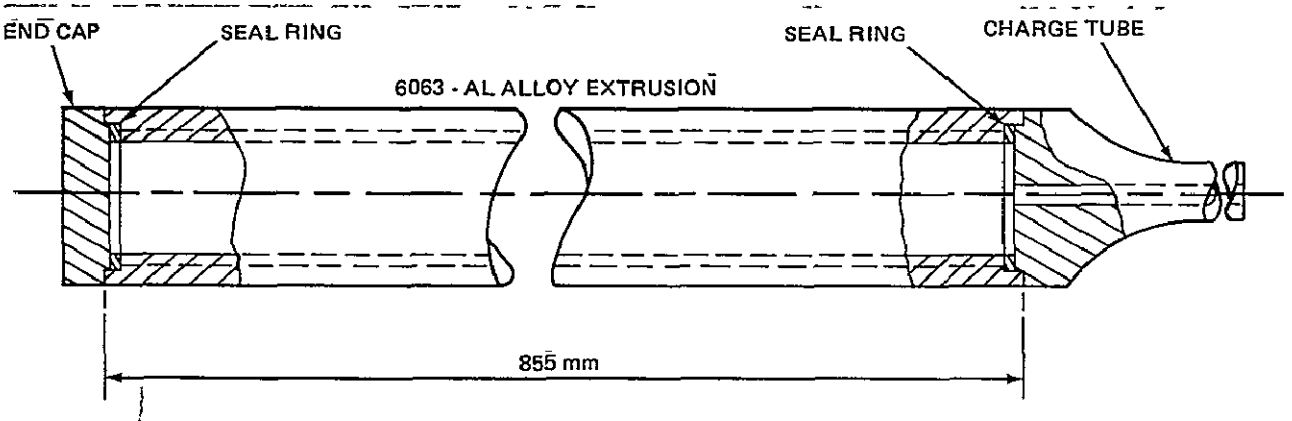

Fig 12 Components of Heat Pipe

After welding on the end fittings, the pipes were sealed under vacuum and heat treated to the T-6 temper with subsequent aging to the T-4 condition. The pipes were then pressure, leak tested with dry nitrogen, helium mixture to 48 atmospheres. Finally, the pipes were baked-out at 100°C under high vacuum and then charged with ultra high purity ammonia.

3.2 Test Procedures

Although two heat pipes were fabricated and charged with ultra high purity ammonia only one of the pipes was tested. A total of four series of tests were completed:

- A check for non-condensible gas
- A performance map (maximum heat transport capability as a function of heat pipe tilt and evaporator, condenser temperature drops as a function of heat transport)
- A limited test series to investigate the effect of non-condensible gas on pumping capability
- A limited test series to investigate the reprriming capability of the pipe from both mechanical and thermal induced dry-out.

The pipe used for these four series of tests was deliberately initially overcharged with 9.2 gm of ammonia and then valved off. The heat pipe was instrumented with a heater and thermocouples, the heater consisting of Nichrome ribbon wrapped helically along the pipe and insulated from the pipe by a half mil layer of double backed kapton tape. This heater, as shown on Figure 13, covered a 305 mm. (12 inch) length of the pipe at the valve end. A total of thirteen copper, constantan thermocouples were strapped to the pipe at the 3 o'clock orientation, the bead being located between consecutive turns of the heater element in the heated zone. The thermocouples were recorded continuously using a multi-point Bristol recorder while the steady-state temperature distributions were recorded using an indicating digital voltmeter. The evaporator and adiabatic zones of the heat pipe plus the valve were insulated with preformed ARMOFLEX insulation. The voltage across the terminals of the heater ribbon was varied by a Variac and the voltage measured using a voltmeter.

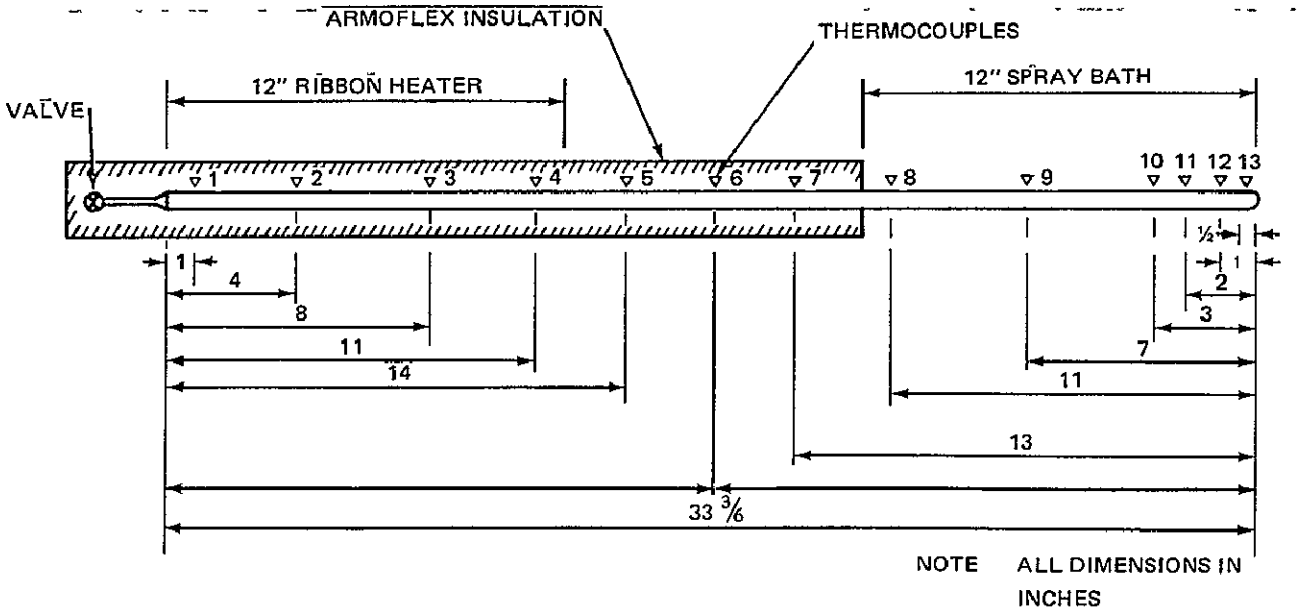

Fig 13 NASA Lewis Covert Groove Heat Pipe Test Instrumentation

Two different heat sinks were used, one for the test series to check for non-condensible gas and the second for all other tests. After charging the pipe with 9.2 gm of ammonia the pipe was checked for the presence of non-condensible gas by operating the pipe in the reboiler mode (5 cm tilt) at -40°C with 40 watts of heater power. The heat sink was a stirred alcohol bath with liquid nitrogen bubbled through it. The recorded temperature profile, as shown on Figure 14, was flat with no indication of non-condensible gas. If gas had been present it would have collected as a gas pocket at the coldest point of the pipe and the pipe wall local to the gas pocket would have run at or close to the sink temperature. One can conclude therefore that gas, if present, occupied less than 12.7 mm. of the pipe at -40°C and at 20°C this gas would have been compressed to less than 1.2 mm. at the end of the condenser.

The heat sink for all other tests consisted of a cold water spray bath. The performance tests consisted of setting the pipe at a predetermined tilt, turning on

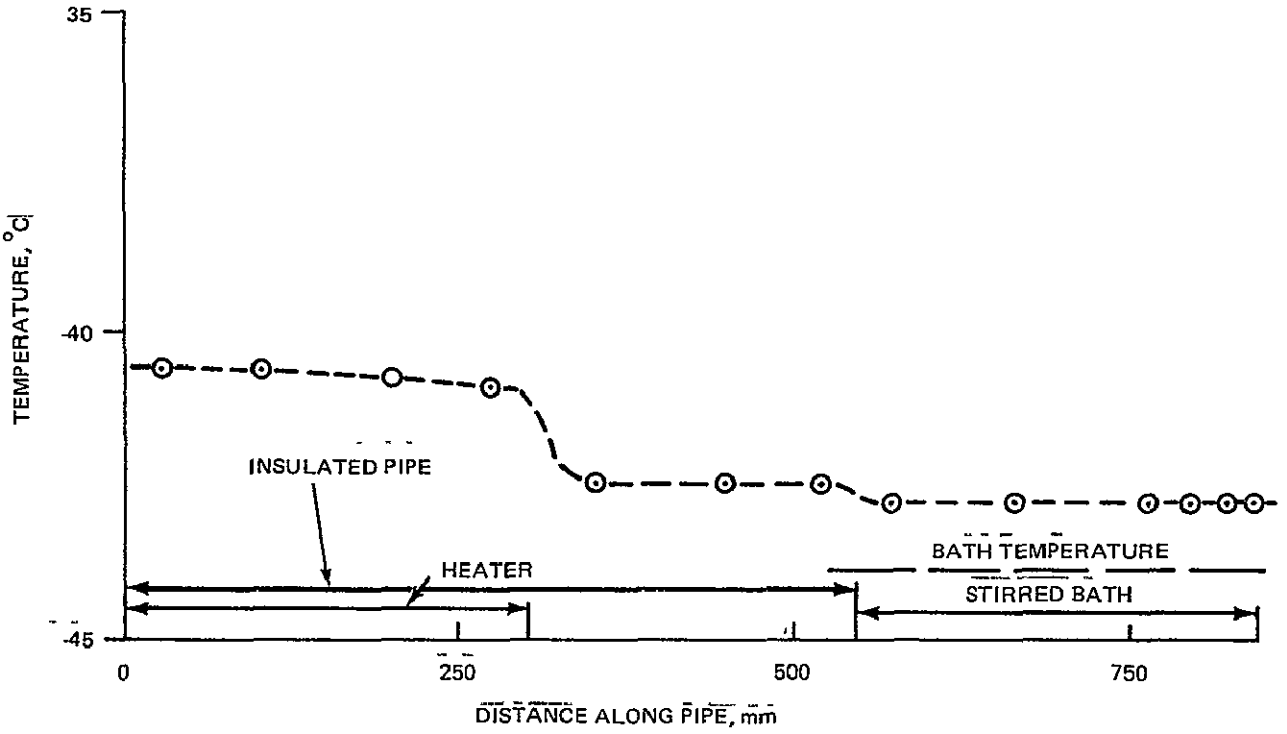

Fig 14 Temperature Distribution Recorded During Initial Test To Check For Non-Condensible Gas

the spray bath and then increasing the heater dissipation in 20 watt increments with a ten minute pause at each power setting. The cooling water flow rate and temperature were adjusted to maintain the adiabatic section of the pipe between 15 and 20°C. The heater power was increased until a run-away dry-out occurred at which point the power was then immediately reduced to zero. The pipe was left for 5 minutes to recover then the power increased to approximately 20 watts below the last dry-out heater dissipation. The power was then increased in five watt increments with the power held constant for 15 minutes at each power setting. At the second indication of run-away dry-out the power was again reduced to zero, the next pipe tilt set and the test repeated. On completing tests at all tilts the charge in the pipe was decreased by opening the valve and venting out some ammonia vapor, care being taken to ensure that no air entered the pipe. The new fluid charge was determined by weighing and then the performance test repeated.

At the completion of the performance test with 6.3 gm ammonia some dry nitrogen was deliberately injected into the heat pipe and the performance test repeated. After this test the pipe was re-evacuated, rebaked-out and then charged with 6.1 gm ammonia. It was anticipated that 6.1 gm ammonia would represent an under-charged condition. The check for non-condensible gas and the performance tests were then repeated.

The pipe was recharged with 6.3 gm ammonia, the non-condensible gas check repeated and sufficient data taken to verify the heat pipe performance. Reprming tests were then completed. This test consisted of elevating the evaporator approximately 180 m.m. (7") above the condenser and leaving the pipe at this tilt for at least 15 minutes to allow the grooves to drain. The cooling water was then turned-on, the pipe tilt quickly reduced to 12 mm. (1/2 inch) and the heater immediately enabled. This test was performed at 25w, 40w, 50w and then 60 watts of heater dissipation. Finally, the test was repeated but this time the heater was enabled at 15 watts while the pipe was tilted 180 mm. (7 inch). When the pipe temperature in the evaporator reached 50°C the pipe elevation was quickly reduced to 12 mm. and the power immediately increased to 25, 40, 50 or 60 watts.

3.3 Experimental Results

The test data for the performance tests were examined for incipient dry-out by plotting the evaporator temperature difference against heater disipation, the evaporator temperature difference being defined as the difference in temperature between the end evaporator thermocouple (T/C #1) and the average of the three thermocouples (#5, 6, and 7) in the adiabatic section. The data indicated a linear change in temperature difference with heat input with a very sharply defined incipient dry-out point. All data recorded below the incipient dry-out condition at each heat pipe tilt has been presented in Figure 15, the evaporator, condenser and overall temperature differences being based upon the average temperatures in each region of the pipe,

$$\Delta T_{EVAP} = \bar{T}_{EVAP} - \bar{T}_{ADIA}$$

$$\Delta T_{COND} = \bar{T}_{ADIA} - \bar{T}_{COND}$$

$$\Delta T_{OVERALL} = \bar{T}_{EVAP} - \bar{T}_{COND}$$

The data are shown for all tilts and heater dissipations below dry-out. There is an obvious effect of charge condition on both the evaporator and condenser temperature drops. The dependence of the condenser temperature drop on charge was not unexpected; the puddle reduces the area available for condensation hence, the temperature drop should increase with increasing charge at constant heater dissipation. However, increasing tilt at constant charge also reduces the surface area covered by the puddle and one would expect the temperature drop to decrease with increasing tilt at constant heater dissipation and fluid charge. No trend with tilt was detected. The dependency of the evaporator temperature drop on charge is more difficult to explain but can be qualitatively explained by the local change in meniscus profile due to the puddle extending along the pipe. A long puddle would result in a flatter meniscus at the start of the evaporator than a short puddle. As heat transfer in the evaporator occurs through the meniscus liquid film local to the solid boundary then the thick flat meniscus should result in a higher temperature drop (lower film coefficient)

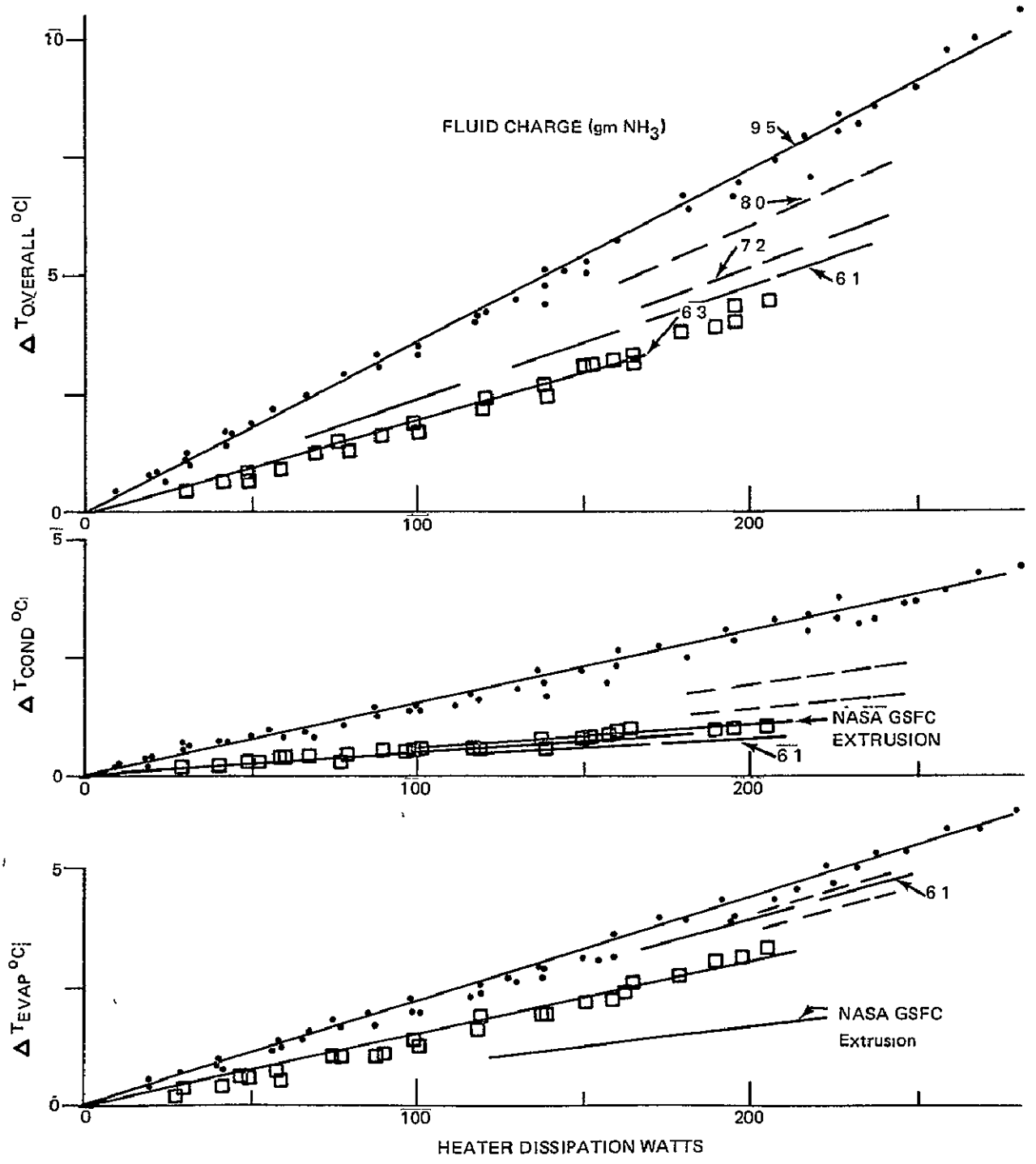

Fig 15 Heat Pipe Temperature Difference as a Function of Heat Transport and Fluid Charge

than the thinner more depressed meniscus associated with a lower fluid charge. However, this effect should also be somewhat tilt dependent. No dependency with tilt was observed for the test data. The 6.1 gm ammonia charge represents an under-charge condition. With this charge the meniscus retreats into the circular section of the groove and hence the evaporator film coefficient is less than the coefficient with 6.3 gm ammonia. In the condenser the condensate immediately runs into the groove, the film thickness is slightly thinner than in the 100% charge condition; there is slightly greater area available for condensation to occur, hence, the condenser film coefficient is higher than in the 100% charge.

The puddle formation in the overcharged pipes is not representative of zero-g excess liquid slug formation. The heat transfer coefficient for zero-g application must therefore be based upon the test data obtained with 100% charge i.e. 6.3 gm ammonia. The film coefficients based upon the pipe core diameter were calculated from the test data as

evaporator film coefficient 7300 $W/M^2{}^oC$ (1300 BTU/HR $Ft^2{}^oF$)

condenser film coefficient 20,500 $W/M^2{}^oC$ (3600 BTU/HR $Ft^2{}^oF$)

For comparison the corresponding values for the NASA GSFC extrusion, computed from unreported Grumman test data, are evaporator coefficient 11,600 $W/M^2{}^oC$ (2100 BTU/HR $Ft^2{}^oF$) and condenser coefficient 16,800 $W/M^2{}^oC$ (2950 BTU/HR $Ft^2{}^oF$). The ratio of the evaporator coefficients (GSFC to LEWIS: 11,600 to 7300) is approximately equal to the ratio of the number of grooves (27/20). This supports the generally held view that the heat transfer in the evaporator occurs local to the meniscus attachment point and should therefore be a function of the number of grooves rather than total groove or land width. Condensation is generally held to occur on the fin lands with subsequent drainage into the grooves. Two parameters are important, the total land area and the land area per groove (this second parameter controls the condensate film thickness). The Lewis extrusion has approximately double the total land area and 2.7 times the land area/groove compared to the GSFC extrusion. No simple analysis is possible to determine the net effect of these two parameters. The test data does however

suggest that the total land area is more important than the land area/groove.

The heat transport capability of the pipe is summarized in Figure 16 as the maximum heat transport limit as a function of heat pipe tilt. On this figure two values are plotted for each fluid-charge, heat-pipe tilt point, the maximum heat transport

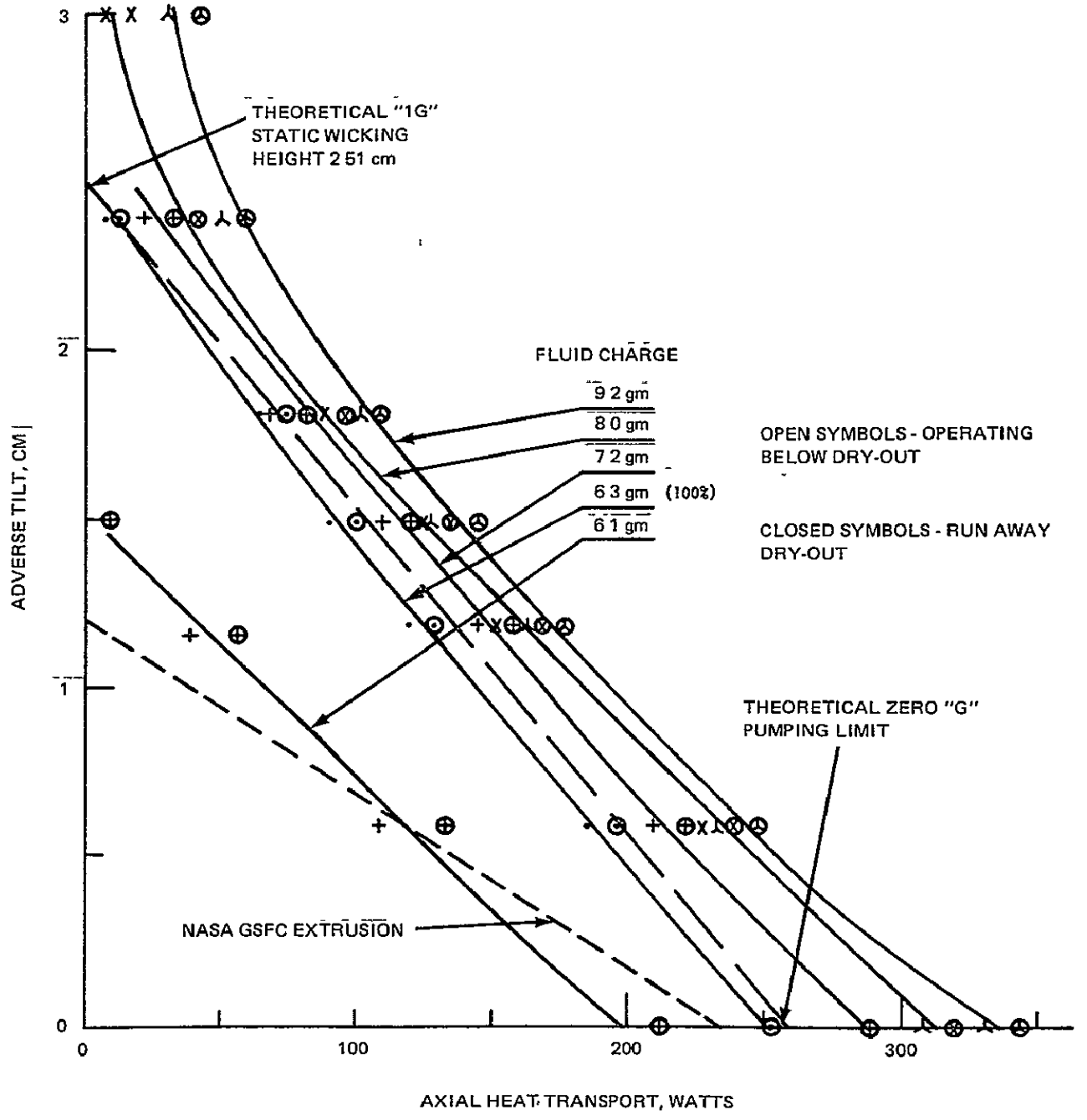

Fig 16 Performance Limit as a Function of Adverse Tilt

recorded with the pipe operating and then the power at which run-away dry-out was observed. As one would expect, the maximum transport capability at constant tilt decreased with decreasing fluid inventory. The concave shape of the performance curves with overcharged pipes is typical of grooved heat pipe data and is due to the puddle decreasing the effective length of the condensate return path. On reducing the fluid charge from 6.3 gm to 6.15 gm the performance fell-off dramatically, indicating a transition from fully charged to an undercharged condition. The vapor temperature (or adiabatic section of the pipe) was maintained in the range 15°C to 20°C. Assuming an average temperature of 18°C the computed 100% fluid charge condition corresponds to 6.22 gm ammonia. The 100% fluid charge calculation is therefore validated by the test data.

Also shown in Figure 16 is the line joining the zero "g" predicted performance point to the static wicking height. These two points can be considered as, (1) the pumping capability of the pipe in one "g" at zero tilt, if puddle flow can be eliminated (that is, no overfill or no groove drainage) and (2) the tilt at which the pumping capability decreases to zero, again assuming the puddle can be eliminated. The predicted performance limit is in excellent agreement with the test data. Finally on Figure 16, the test data for a heat pipe manufactured from the NASA GSFC extrusion are summarized. The Lewis extrusion has a slightly higher zero tilt pumping capability and approximately double the static wicking height when compared to the NASA GSFC extrusion. In these respects, the Lewis extrusion has superior ground test characteristics. In addition it must be noted that the Lewis extrusion requires only approximately 67% of the ammonia charge required by the GSFC extrusion. This means that although the Lewis extrusion is very sensitive to undercharge it is less sensitive to overcharge, a 6% overcharge is equivalent (in zero-g) to a liquid slug filling 1% of the pipe. With the GSFC extrusion a 6% overcharge would result in a liquid slug filling 2.1% of the pipe.

The effect of deliberably injecting some dry-nitrogen into the pipe is shown in Figure 17. The gas converted the heat pipe into a reservoirless VCHP. At 15°C the gas occupied part of the condenser decreasing the effective pipe length by approximately 15% at dry-out. As noted with other grooved VCHP's, the presence of the gas

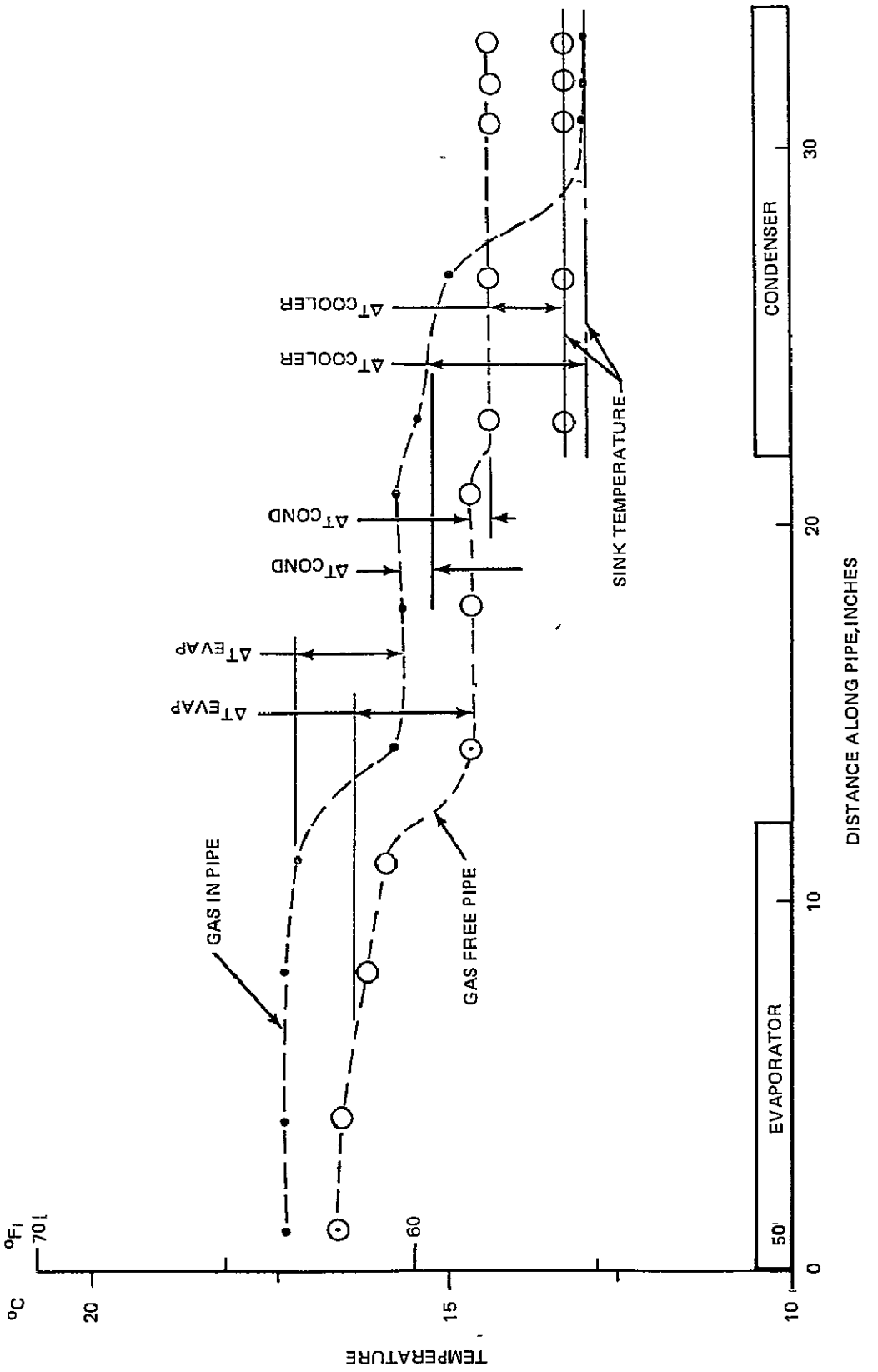

Fig 17 Comparison of Temperature Profile Along Pipe With and Without Inert Gas

decreased the maximum watt meter transport capability of the heat pipe but maintained the same maximum axial heat transport. Although the reason for the reduction in Qdx is not well understood at the present time, the fact that Qmax is not reduced makes this more of an academic than a practical problem. The NASA Lewis extrusion should be perfectly acceptable for gas loaded VCHP's. The effect of gas has been well documented for arterial heat pipes, where the degraded performance has been attributed to gas blockage of some of the arteries. Severe degradation has been experienced which has limited the application of artery VCHP's, especially with ammonia.

The reprimimg tests were intended to investigate the rate at which the pipe would recover due to a mechanical or a mechanical/thermal deprimimg sequence. The mechanical deprimimg, for example, would be equivalent to despinning a spacecraft soon after launch before any temperature gradients could be set up. The mechanical, thermal deprime would correspond to despinning a spacecraft after temperature gradients had been established. The test data are summarized in Figures 18 and 19. In Figure 18 the reprimimg of the pipes (under load) from a purely mechanical deprime are compared for 25w, 40w and 50w heater powers. In all cases the pipe quickly primed and operated as an isothermalizer. One further test was carried out in this series with 60 watts of heater power. The last thermocouple on the evaporator (#1) did not fully recover and was some 15°C above the rest of the pipe 15 minutes after decreasing the pipe tilt to 12mm. The heat transport limit for this tilt from Figure 16 is 140 watts. The inability to reprime at 60 watts is therefore not a simple transport limit. Possible mechanisms are poor surface wetting (perhaps related to boiling heat transfer) or upper grooves not priming. On Figure 19 repriming after a mechanical, thermal dry-out is compared to reprimimg after a pure mechanical dry-out. At 40 watts dissipation the pipe quickly primed from both dry-out conditions. At 50 watts the pipe took 25 minutes to recover after the mechanical, thermal dry-out. At 60 watts the pipe did not recover after the mechanical, thermal dry-out.

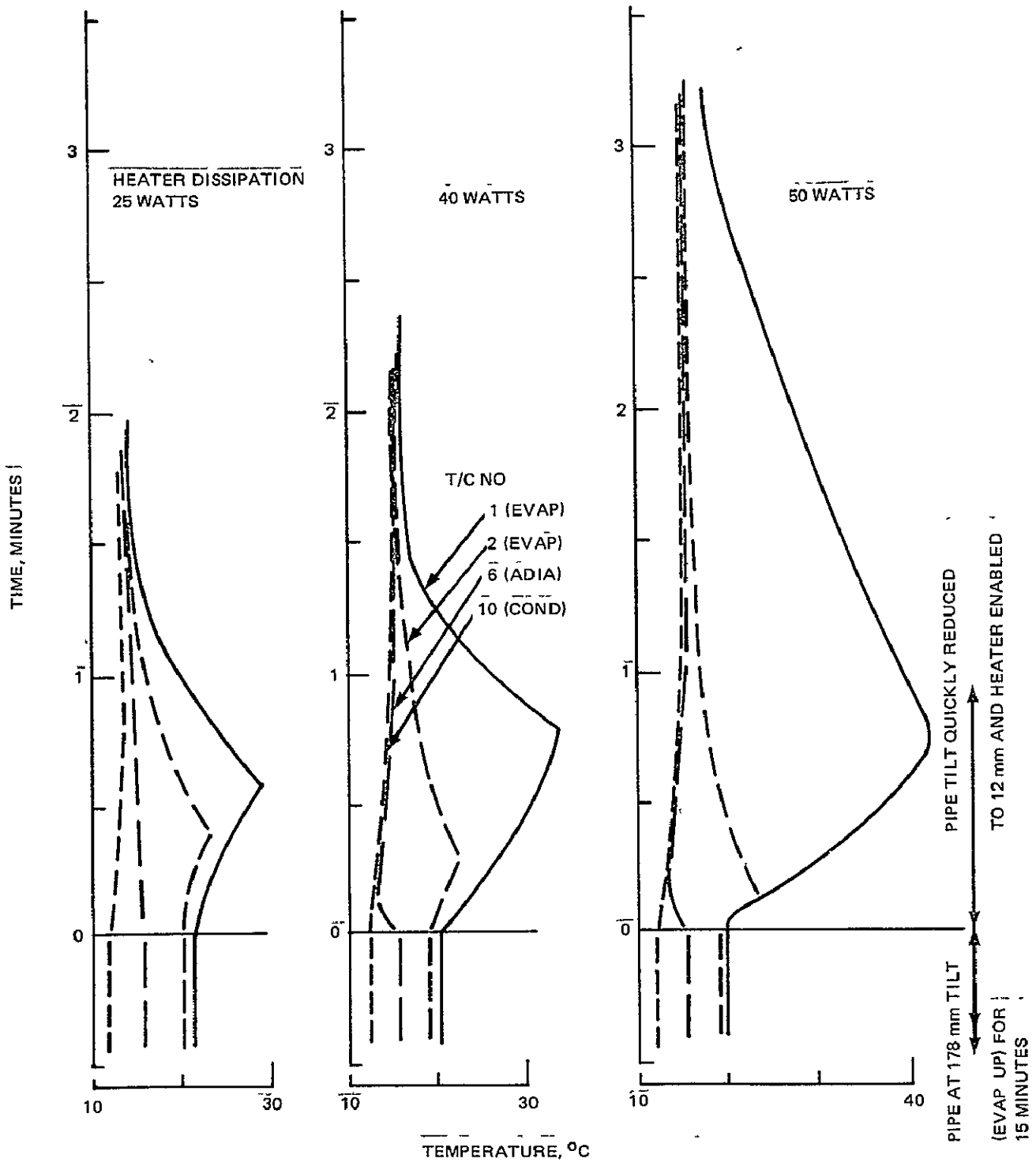

Fig 18 Repriming From A Mechanically Induced Dry-Out

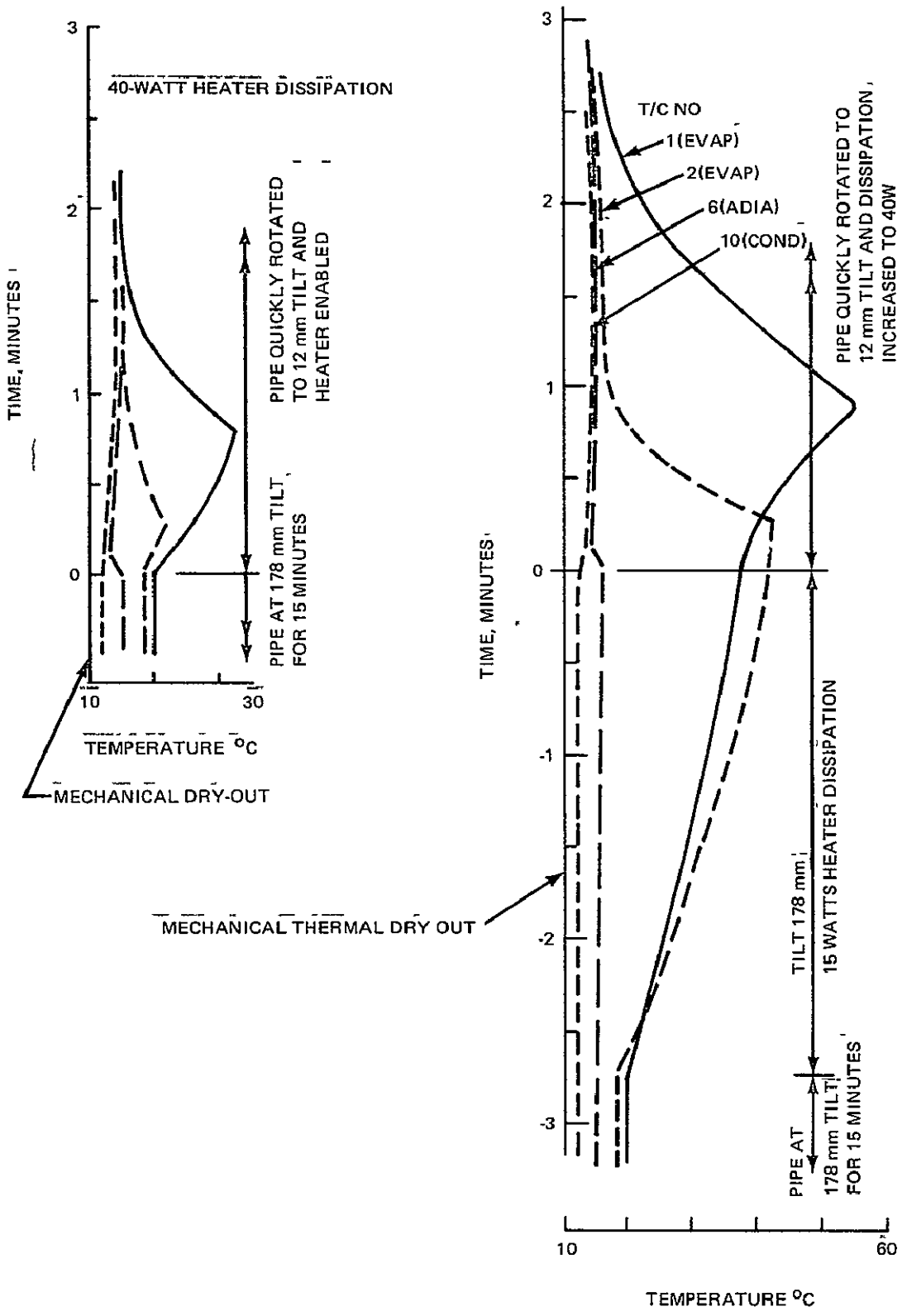

Fig 19 Comparison of Reprimng From A Mechanical and A Mechanical/Thermal Dry-Out

4 CONCLUSIONS

Examination of the Lewis extrusion both visually and by measurement showed that the extrusion had no discernible rifling and little variation in groove geometry both circumferentially (groove to groove) and axially (along a groove). The groove dimensions were very close to the original trade-off design values, an excellent recommendation for the accuracy of the extrusion process. The main disadvantage with this particular extrusion is the thin wall; the pipe OD was fixed by the available condenser and heater blocks of the Lewis test fixtures, the pipe ID was limited by fabrication of the extrusion mandrel. The fabricators of the extrusion (Micro Extrusions) are confident, however, that the extrusion can be produced with a thicker wall (larger O.D.). A thicker wall combined with heat treatment after welding would allow this extrusion to be used in any application envisaged for an extruded aluminum heat pipe.

The analytical predictions of transport capability are in excellent agreement with the experimental data and confirm the original trade-off studies which predicted the superior capability of the covert groove extrusion. The measured evaporator and condenser film coefficients with ammonia are also in good agreement with what one would have predicted from data recorded from the NASA GSFC extrusion the values being

- evaporator coefficient 7300 $W/M^2{}^oC$ (1300 BTU/Hr $Ft^2{}^oF$)
- condenser coefficient 20,500 $W/M^2{}^oC$ (3600 BTU/Hr $Ft^2{}^oF$)

Other relevant data are

- static wicking height (at 20^oC) 2.51 cm
- zero gravity pumping limit (at 20^oC) 143 w.m. (5700 watt inches)
- fluid charge (at -20^oC) 7.3 gm/meter length of pipe

These test data and theoretical predictions indicate that the Lewis extrusion would be an excellent candidate for any axially grooved heat pipe application in which an aluminum pipe could be used. Potential fluids are ammonia, butane, ethane, methane, hydrogen.

5. REFERENCES

1. Gaugler, R.S., "Capillary Heat Transfer Devices for Refrigerating Apparatus", U.S.A. Patent 2,448,261 (Disclosure Date April 30, 1945).

2. Thompson, D.C., Patent Disclosure 48148 February 10, 1960.

3. Grover, G.M., Cotter, T.P., Erickson, G.F., "Structures of Very High Thermal Conductance", Journal of Applied Physics, 35, 1990, (1964).

4. Cotter, T.P., "Theory of Heat Pipes" LA-3246-MS, Los Alamos Scientific Laboratory, 1965.

5. Parker, G.H., Hanson, J.P., "Heat Pipe Analysis" 1967 Intersociety Energy Conversion Conference.

6. Frank, S., "Optimization of Grooved Heat Pipe", 1967 Intersociety Energy Conversion Conference.

7. "Fill Determination Study of ATS-F and G Heat Pipes", Summary Report DTM-72-12 by Dynatherm Corporation.

8. Kosowski, N., Kosson, R., "Experimental Performance of Grooved Heat Pipes at Moderate Temperatures", AIAA Paper 71-409.

9. Bilenas, J., Harwell, W., "OAO Heat Pipes - Design Analysis and Testing", ASME Paper 70-HT/SpT-9.

10. Schlitt, K.R., Kirkpatrick, J.P., Brennan, P.J., "Parametric Performance of Extruded Axial Grooved Heat Pipes from 100 to 300 K." AIAA Paper 74-724.

11. McIntosh, R., Ollendorf, S., Harwell, W., "International Heat Pipe Experiment" AIAA Paper 75-726

12. Harwell, W., Edelstein, F., McIntosh, R., and Ollendorf, S., "Orbiting Astronomical Observatory Heat Pipe Flight Performance Data", AIAA Paper 73-758.

13. Berger, M.D., and Kelly, W.H., "Application of Heat Pipes to the ATS-F Spacecraft", ASME Paper 75-ENAS-46.

14. Eggers, P.E., Private Communication. Battelle Memorial Institute, Ohio.

APPENDIX

A1. PERFORMANCE MAP

The object of the computer code is to determine the performance map for a given groove profile, temperature level and fluid. See Fig. 4 (Section 2.2) for a typical performance map.

The program starts by assuming a heat flow along the pipe with an assumed radius of curvature of the meniscus at the end of the evaporator. A numerical integration is performed along the pipe with a check at each iteration to ensure that the radius of curvature of the meniscus does not exceed the assumed maximum value of $100*R_{min}$.

The program is set-up to automatically increment the meniscus radius in the evaporator in steps

$$R = \frac{WT}{2\cos\theta} * F$$

where WT is groove opening

θ is groove taper

F is a multiplication factor which assumes values of 1.0, 1.05, 1.15 and 1.30.

The axial heat flow is also automatically incremented in steps, to assume values of,

2.5, 5.0, 7.5, 10, (+10) watts

If the pumping limit is exceeded with the assumed axial heat flow of 10 watts or less the heat flow is decreased by 1.25 watts and the calculation repeated. The program then searches for a new temperature or groove data. At axial heat flows greater than 10 watts a factor DELTA is calculated

$$DELTA = R_{min}/(R_{cond} - R_{min}) * QH$$

where QH is the last assumed axial heat flow rate,

R_{min} is the assumed minimum radius of curvature and,

R_{cond} is the radius of curvature in the condenser corresponding to QH.

If DELTA is greater than 10 then QH is incremented by 10. If DELTA is less than 10 then QH is incremented by 85% of DELTA. The 85% factor is to ensure that the pumping limit is not exceeded. The next time around the loop the program increments the initial radius of curvature in the evaporator and returns to QH = 2.5 watts.

A 2 INPUT DATA

Card #

1 Title 18A4

2 DO, DR, DC, WALL 4E12.5

DO, PIPE OD (Inches)

DR, ROOT Dia (Inches)

DC, CORE Dia (Inches)

WALL, WALL THK (Inches)

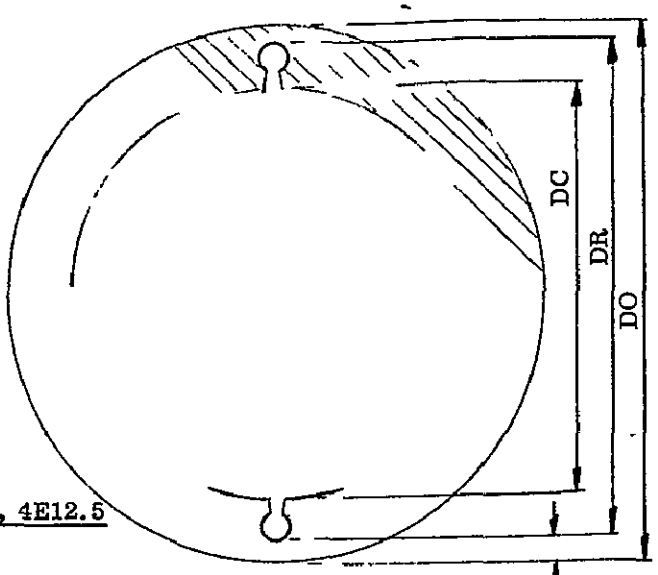

3 NG, DG, WT, WB, THETA1 I4, 4E12.5

NG, Number of Grooves

DG, Groove Dia (Inches)

WT, Groove Tip Opening (Inches)

WB, Groove Base Opening (Inches)

THETA1, Entrance Passage Taper (Degs)

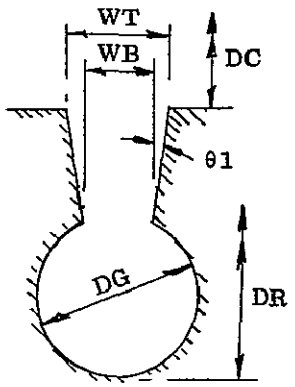

4 XLE, XLA, XLC 3E12.5

XLE, Evaporator Length (Inches)

XLA, Adiabatic Length (Inches)

XLC, Condenser Length (Inches)

5 Fluid, Tempc, Nutemp, Nugrov 2E12.5, 2I4

Fluid, ID Number
1. Ammonia
2. Methane
3. Ethane
4. Propane
5. Butane

Tempc, Operating Temp ^{o}C

Nutemp, Replacement Data *

Nugrov, Replacement Data *

* Integer ≥ 1 will send program back to look for new Tempc or groove geometry.

CMOD EQUALS.10000F 01
$$$$$$$$$$$$$

TEMP DEG C	HEAT INPUT WATTS	TRANSPORT WATT.IN	VAP REY NO	CHARGE GRAMS	DELTA AREA %AT
0.0	0.25000E 01	0.54375E 02	0.29575E 02	0.62972E 01	-0.21898E-03
0.0	0.50000E 01	0.10875E 03	0.59151E 02	0.62982E 01	-0.21898E-03
0.0	0.75000E 01	0.16313E 03	0.88726E 02	0.62991E 01	-0.24635E-03
0.0	0.10000E 02	0.21750E 03	0.11830E 03	0.63000E 01	-0.16423E-03
0.0	0.20000E 02	0.43500E 03	0.23660E 03	0.63036E 01	-0.19160E-03
0.0	0.30000E 02	0.65250E 03	0.35490E 03	0.63070E 01	-0.21898E-03
0.0	0.40000E 02	0.87000E 03	0.47321E 03	0.63102E 01	-0.21898E-03
0.0	0.50000E 02	0.10875E 04	0.59151E 03	0.63133E 01	-0.21898E-03
0.0	0.60000E 02	0.13050E 04	0.70981E 03	0.63162E 01	-0.21898E-03
0.0	0.70000E 02	0.15225E 04	0.82811E 03	0.63190E 01	-0.21898E-03
0.0	0.80000E 02	0.17400E 04	0.94641E 03	0.63218E 01	-0.21898E-03
0.0	0.90000E 02	0.19575E 04	0.10647E 04	0.63244E 01	-0.21898E-03
0.0	0.10000E 03	0.21750E 04	0.11830E 04	0.63269E 01	-0.19160E-03
0.0	0.11000E 03	0.23925E 04	0.13013E 04	0.63294E 01	-0.19160E-03
0.0	0.12000E 03	0.26100E 04	0.14196E 04	0.63317E 01	-0.27372E-03
0.0	0.13000E 03	0.28275E 04	0.15379E 04	0.63341E 01	-0.21898E-03
0.0	0.14000E 03	0.30450E 04	0.16562E 04	0.63363E 01	-0.24635E-03
0.0	0.15000E 03	0.32625E 04	0.17745E 04	0.63386E 01	-0.21898E-03
0.0	0.16000E 03	0.34800E 04	0.18928E 04	0.63407E 01	-0.21898E-03
0.0	0.17000E 03	0.36975E 04	0.20111E 04	0.63428E 01	-0.21898E-03
0.0	0.18000E 03	0.39150E 04	0.21294E 04	0.63449E 01	-0.21898E-03
0.0	0.19000E 03	0.41325E 04	0.22477E 04	0.63470E 01	-0.24635E-03
0.0	0.20000E 03	0.43500E 04	0.23660E 04	0.63490E 01	-0.24635E-03
0.0	0.21000E 03	0.45675E 04	0.24843E 04	0.63510E 01	-0.21898E-03
0.0	0.22000E 03	0.47850E 04	0.26026E 04	0.63530E 01	-0.21898E-03
0.0	0.23000E 03	0.50025E 04	0.27209E 04	0.63550E 01	-0.19160E-03
0.0	0.24000E 03	0.52200E 04	0.28392E 04	0.63570E 01	-0.21898E-03
0.0	0.25000E 03	0.54375E 04	0.29575E 04	0.63589E 01	-0.27372E-03
0.0	0.26000E 03	0.56550E 04	0.30758E 04	0.63608E 01	-0.21898E-03
0.0	0.27000E 03	0.58725E 04	0.31941E 04	0.63628E 01	-0.24635E-03
0.0	0.28000E 03	0.60900E 04	0.33124E 04	0.63647E 01	-0.19160E-03
0.0	0.29000E 03	0.63075E 04	0.34307E 04	0.63666E 01	-0.24635E-03
0.0	0.30000E 03	0.65250E 04	0.35490E 04	0.63685E 01	-0.21898E-03
0.0	0.31000E 03	0.67425E 04	0.36673E 04	0.63704E 01	-0.19160E-03
0.0	0.32000E 03	0.69600E 04	0.37856E 04	0.63723E 01	-0.21898E-03

HEAT PIPE CANNOT PUMP 0.32710E 03 WATTS AT 0.0 DEG C

HEAT PIPE CANNOT PUMP 0.32585E 03 WATTS AT 0.0 DEG C

CMOD EQUALS.10500F 01
$$$$$$$$$$$$$

TEMP DEG C	HEAT INPUT WATTS	TRANSPORT WATT.IN	VAP REY NO	CHARGE GRAMS	DELTA AREA %AT
0.0	0.25000E 01	0.54375E 02	0.29575E 02	0.63088E 01	-0.21898E-03
0.0	0.50000E 01	0.10875E 03	0.59151E 02	0.63096E 01	-0.21898E-03
0.0	0.75000E 01	0.16313E 03	0.88726E 02	0.63104E 01	-0.21898E-03
0.0	0.10000E 02	0.21750E 03	0.11830E 03	0.63113E 01	-0.21898E-03
0.0	0.20000E 02	0.43500E 03	0.23660E 03	0.63144E 01	-0.21898E-03
0.0	0.30000E 02	0.65250E 03	0.35490E 03	0.63175E 01	-0.21898E-03
0.0	0.40000E 02	0.87000E 03	0.47321E 03	0.63204E 01	-0.21898E-03
0.0	0.50000E 02	0.10875E 04	0.59151E 03	0.63232E 01	-0.24635E-03
0.0	0.60000E 02	0.13050E 04	0.70981E 03	0.63258E 01	-0.19160E-03
0.0	0.70000E 02	0.15225E 04	0.82811E 03	0.63284E 01	-0.19160E-03
0.0	0.80000E 02	0.17400E 04	0.94641E 03	0.63309E 01	-0.19160E-03

A.3 TYPICAL OUTPUT DATA

```
   LEWIS/NASA RE-ENTRANT GROOVE HEAT PIPE

$$$$      INPUT DATA      $$$$$

   PIPE DIA      ROOT DIA      CORE DIA      WALL THK
      INCH          INCH          INCH          INCH
0.49880E 00 0.44770E 00 0.36540E 00 0.25200E-01

NO GROOVES  GROOVE DIA  GROOVE TIP  GROOVE BASE  ENT TAPER
              INCH          INCH         INCH      DEGREES
        20  0.31700E-01 0.10500E-01 0.86000E-02 0.57500E 01

  EVAP LEN     ADIA LEN     COND LEN    TOTAL LEN
     INCH         INCH         INCH         INCH
0.12000E 02 0.97500E 01 0.12000E 02 0.33750E 02


  CALC PIPE THK IS 0.25550E-01 INCHES AT ROOT OF GROOVE

  CALC GAP TAPER IS 0.54030E 01 DEGS COMPARED TO  0.57500E 01 DEGS MEASURED


   BASED ON FLAT MENISCUS
  CALCULATED GROOVE AREA PLUS ENTRANCE PASSAGE
       0.17635E-01 SQ IN ( 0.15716E-01 PLUS 0.19185E-02)
  CALCULATED CORE AREA
      0.10485E 00 SQ IN


    LIQUID IS AMMONIA

     TEMPE         PRESS        LIQDEN        VAPDEN        LIQVIS        VAPVIS
     DEG F          PSIA         LB/FT3        LB/FT3      LBM/FTHR      LBM/FTHR
0.32000E 02 0.62088E 02 0.39884E 02 0.21428E 00 0.40730E 00 0.22190E-01

     SURTEN        LAT HT         F.O.M        RISE F        GAMMA         MOL WT
     LBF/FT       BTU/LB       BTU/FT2HR      SQ IN
0.17805E-02 0.54364E 03 0.39554E 11 0.64284E-02 0.13360E 01 0.17032E 02


 COMPLETELY FLAT MENISCUS CONTACTING LANDS CHARGE IS  0.64359E 01 GRAMS

 SONIC VELOCITY 0.13852E 04 FT/SEC( 0.42221E 03 M/S)

 SONIC HEAT FLUX 0.54699E 06 W/SQ IN ( 0.84783E 09 W/SQ M)

 ENTRAINMENT LIMIT 0.22862E 05 W/SQ IN ( 0.35435E 08 W/SQ M)

 BASED ON OPERATIONAL MODE 1(MENISCUS ATTACHED TO LANDS  AT ALL POINTS)
 STATIC WICKING HEIGHT 0.12190E 01  INCH ( 0.30963E-01 M)
 STATIC WICKING HEIGHT IS 0.45316E-01 PERCENT OF PIPE PRESSURE
```